NUCLEAR ENGINEERING

MASSACHUSETTS INSTITUTE OF TECHNOLOGY

DISCLAIMER

DOE/ET/37240-89

COOLANT MIXING IN LMFBR ROD BUNDLES AND OUTLET PLENUM MIXING TRANSIENTS

P.I.: Neil E. Todreas - Tasks I and II
Michael W. Golay - Task III
Lothar Wolf - Task IV

PROGRESS REPORT
September 1, 1980-November 30, 1980

Report No. DOE/ET/37240-89
February 1981

MGW

REPORTS AND PAPERS PUBLISHED UNDER MIT COOLANT MIXING IN LMFBR ROD BUNDLES PROJECT

A. Quarterly Progress Reports (Available from:
National Technical Information Service
U. S. Department of Commerce
Springfield, Virginia 22151)

COO-2245-1	Period June 1, 1972 - November 30, 1972
COO-2245-2	Period December 1, 1972 - February 28, 1973
COO-2245-3	Period March 1, 1973 - May 31, 1973
COO-2245-6	Period June 1, 1973 - August 31, 1973
COO-2245-7	Period September 1, 1973 - November 30, 1973
COO-2245-8	Period December 1, 1973 - February 28, 1974
COO-2245-10	Period March 1, 1974 - May 31, 1974
COO-2245-13	Period June 1, 1974 - August 31, 1974
COO-2245-14	Period September 1, 1974 - November 30, 1974
COO-2245-15	Period December 1, 1974 - February 28, 1975
COO-2245-23	Period March 1, 1975 - May 31, 1975
COO-2245-25	Period June 1, 1975 - August 31, 1975
COO-2245-26	Period September 1, 1975 - November 30, 1975
COO-2245-28	Period December 1, 1975 - February 29, 1976
COO-2245-30	Period March 1, 1976 - May 31, 1976
COO-2245-31	Period June 1, 1976 - August 31, 1976
COO-2245-34	Period September 1, 1976 - November 30, 1976
COO-2245-38	Period December 1, 1976 - February 28, 1977
COO-2245-50	Period March 1, 1977 - May 31, 1977
COO-2245-53	Period June 1, 1977 - August 31, 1977
COO-2245-60	Period September 1, 1977 - November 30, 1977
COO-2245-63	Period December 1, 1977 - February 28, 1978
COO-2245-64	Period March 1, 1978 - May 31, 1978
COO-2245-65	Period June 1, 1978 - August 31, 1978
COO-2245-66	Period September 1, 1978 - November 30, 1978

COO-2245-69 Period December 1, 1978 - February 28, 1979

COO-2245-70 Period March 1, 1979 - May 31, 1979

COO-2245-71 Period June 1, 1979 - August 31, 1979

COO-2245-72 Period September 1, 1979 - November 30, 1979

DOE/ET/37240-75 Period December 1, 1979 - February 29, 1980

DOE/ET-37240-76 Period March 1, 1980 - May 31, 1980

DOE/ET-37240-85 Period June 1, 1980 - August 31, 1980

DOE/ET-37240-89 Period September 1, 1980-November 30, 1980

Reports Issued Under This Contract

B.1 Original Topical Reports (Available from National Technical Information Service, U.S. Department of Commerce, Springfield, VA 22151)

E. Khan and N. Todreas, "A Review of Recent Analytical and Experimental Studies Applicable to LMFBR Fuel and Blanket Assembly Design", COO-2245-4TR, MIT, September 1973.

E. Khan, W. Rohsenow, A. Sonin and N. Todreas, "A Simplified Approach for Predicting Temperature Distribution in Wire Wrapped Assemblies", COO-2245-5TR, MIT, September 1973.

T. Eaton and N. Todreas, "Instrumentation Methods for Interchannel Coolant Mixing Studies in Wire-Wrap Spaced Nuclear Fuel Assemblies", COO-2245-9TR, MIT, June 1974.

Y. B. Chen, K. Ip, N. E. Todreas, "Velocity Measurements in Edge Subchannels of Wire Wrapped LMFBR Fuel Assemblies", COO-2245-11TR, MIT, September 1974.

E. Khan, N. Todreas, W. Rohsenow, A. A. Sonin, "Analysis of Mixing Data Relevant to Wire-Wrapped Fuel Assembly Thermal-Hydraulic Design", COO-2245-12TR, MIT, September 1974.

E. Khan, W. Rohsenow, A. Sonin, N. Todreas, "A Porous Body Model for Predicting Temperature Distributions in Wire Wrapped Fuel and Blanket Assemblies of an LMFBR", COO-2245-16TR, MIT, June 1975.

* E. Khan, W. M. Rohsenow, A. Sonin, N. Todreas, "Input Parameters to the ENERGY Code (To be used with the ENERGY Codes Manual), COO-2245-17TR, MIT, May 1975.

* E. Khan, W. Rohsenow, A. Sonin, N. Todreas, "Manual for ENERGY Codes I, II, III", COO-2245-18TR, MIT, May 1975.

P. Carajilescov and N. Todreas, "Experimental and Analytical Study of Axial Turbulent Flows in an Interion Subchannel of a Bare Rod Bundle", COO-2245-19TR, MIT.

* B. Chen and N. Todreas, "Prediction of Coolant Temperature Field in a Breeder Reactor Including Interassembly Heat Transfer", COO-2245-20TR, MIT, May 1975.

* Revised - See Section B.2

B.1 Original Topical Reports (Continued)

F. Carre and N. Todreas, "Development of Input Data to ENERGY Code for Analysis of Reactor Fuel Bundles", COO-2245-21TR, MIT, May 1975.

H. Ninokata and N. E. Todreas, "Turbulent Momentum Exchange Coefficients for Reactor Fuel Bundle Analysis", COO-2245-22TR, MIT, June 1975.

R. Anoba and N. Todreas, "Coolant Mixing in LMFBR Rod Buncles and Outlet Plenum Mixing Transients, COO-2245-24TR, MIT, August 1975.

* B. Bosy, "Fabrication Details for Wire Wrapped Fuel Assembly Components", COO-2245-27TR, MIT, November 1975.

Ralph G. Bennett and Michael W. Golay, "Interferometric Investigation of Turbulently Fluctuating Temperature in an LMFBR Outlet Plenum Geometry", COO-2245-29TR, MIT, June 1976.

N. E. Todreas, "Thermal Analysis Methods for LMFBR Wire Wrapped Bundles", COO-2245-32TR, MIT, November 1976.

K. L. Basehore and N. E. Todreas, "Development of Stability Criteria and an Interassembly Conduction Model for the Thermal-Hydraulics Code SUPERENERGY", COO-2245-33TR, MIT, December 1976.

Robert Masterson and Neil E. Todreas, "Analysis of the Feasibility of Implementing an Implicit Temporal Differencing Scheme in the SUPERENERGY Code", COO-2245-35TR, MIT, February 1977.

S. Glazer, C. Chiu and N. Todreas, "Collection and Evaluation of Salt Mixing Data with the Real Time Data Acquisition System", COO-2245-36TR, MIT, April 1977.

B. Mikic, E. U. Khan and N. E. Todreas, "An Approximate Method for Predicting Temperature Distribution in Wire Wrapped Fuel Assemblies of an LMFBR", COO-2245-37TR, MIT, April 1977.

J. T. Hawley, C. Chiu and N. Todreas, "Development of a Technique for Subchannel Flow Rate Measurements in LMFBR Wire Wrapped Assemblies", to be issued as COO-2245-39TR 6/80. Never issued. Replaced by DOE/ET/37240-80TR.

* Revised - See Section B.2

B.1 Original Topical Reports (Continued)

C. Chiu and N. Todreas, "WARD Blanket Assembly Pre-Test Predictions by SUPERENERGY", COO-2245-40TR, MIT, May 1977.

C. Chiu, N. Todreas, W. M. Rohsenow, "Flow Split Measurements in LMFBR Blanket Assemblies", COO-2245-41TR, MIT, April 1978.

C. Chiu, J. Hawley, W. M. Rohsenow and N. Todreas, "Pressure Drop Measurements in Wire Wrapped Blanket Assemblies", COO-2245-42TR, July 1977.

C. Chiu, W. M. Rohsenow and N. Todreas, "Mixing Experiments in LMFBR Wire Wrapped Blanket Assemblies", COO-2245-43TR, April 1978.

Yi Ben Chen and Michael W. Golay, "Coolant Mixing in the LMFBR Outlet Plenum", COO-2245-44TR, June 1977.

J. Kelly and N. Todreas, "Turbulent Interchange in Triangular Array Bare Rod Bundles", COO-2245-45TR, July 1977.

K. L. Basehore and N. E. Todreas, "Assessment of the Need to Incorporate a Variable Swirl Flow Model into the ENERGY Code", COO-2245-46TR, July 1977.

K. L. Basehore and N. Todreas, "Analysis of the Thermal-Hydraulic Behavior in the CRBR Secondary Control Assembly, Including Interassembly Heat Transfer Effects", COO-2245-47TR, July 1977.

J. G. Bartzis and N. E. Todreas, "Hydrodynamic Behavior of a Bare Rod Bundle", COO-2245-48TR, MIT, June 1977.

M. R. Fakori-Monazah and N. E. Todreas, "Measurement and Analysis of Flow Wall Shear Stress in an Interior Subchannel of Triangular Array Rods", COO-2245-49TR, MIT, August 1977.

* A. S. Hanson and N. E. Todreas, "Fluid Mixing Studies in an Hexagonal 61-Pin, Wire-Wrapped Rod Bundle", COO-2245-51TR, MIT, August 1977.

S. Glaser, N. Todreas, W. Rohsenow, and A. Sonin, "TRANSENERGY S - Computer Code for Coolant Temperature Prediction in LMFBR Cores During Transient Events", COO-2245-52TR, MIT, February 1981.

C. Chiu, W. M. Rohsenow, and N. E. Todreas, "Mixing Experiments in an Alternating Wire Wrapped Assembly", COO-2245-54TR, MIT, December 1977.

* Revised - See Section B.2

B.1 Original Topical Reports (Continued)

* C. Chiu, W. M. Rohsenow and N. E. Todreas, "Turbulent Sweeping Flow Mixing Model for Wire Wrapped LMFBR Assemblies", COO-2245-55TR, MIT, April 1978.

* C. Chiu, W. M. Rohsenow and N. E. Todreas, "Flow Split Model for LMFBR Wire Wrapped Assemblies", COO-2245-56TR, MIT, April 1978.

K. Basehore and N. E. Todreas, "SUPERENERGY: Multiassembly Thermal-Hydraulic LMFBR Code". Issued as Topical Report COO-2245-57TR, August 1980.

C-N. Wong and L. Wolf, "A 3-D Slug Flow Heat Transfer Analysis of Coupled Coolant Cells in Finite LMFBR Bundles", COO-2245-58TR, MIT, February 1978.

Roohollah Karimi and L. Wolf, "Two Dimensional Structural Analysis of Reactor Fuel Element Claddings Due to Local Effects", COO-2245-59TR, MIT, April 1978.

Vincent Manno and Michael Golay, "Measurement of Heat and Momentum Eddy Diffusivities in Recirculating LMFBR Outlet Plenum Flows", COO-2245-61TR, MIT, June 1978.

* Hafeez Khan, Chong Chiu and Neil Todreas, "Laboratory Manual for Salt Mixing Test in Rod Bundles", COO-2245-62TR, MIT, October 1978.

J. Y. Kim and L. Wolf, "Fully-Developed Mixed Convection Heat Transfer and Pressure Drop in Characteristic Coolant Cells of Finite Hexagonal Bare Bundles", COO-2245-67TR, MIT, Dec. 1978.

M. K. Yeung and L. Wolf, "A Multicell Slug Flow Heat Transfer Analysis of Finite LMFBR Bundles", COO-2245-68TR, MIT, December 1978.

S. F. Wang, W. M. Rohsenow, N. E. Todreas, "Steady, Laminar, Fully-Developed Mixed Convection in Finite Rod Arrays", DOE/ET/37240-73TR, Feb. 1981.

P. D. Symolon, N. E. Todreas, "A Manual for Use with the Computer Code Superenergy-Data Reduction Version", COO-2245-74TR, MIT, February 1980.

K. J. Burns, N. E. Todreas, "Laboratory Manual for Static Pressure Drop Experiments in LMFBR Wire Wrapped Rod Bundles", DOE/ET/37240-77TR, July 1980.

K. J. Burns, N. E. Todreas, "A Comparison Between the SIMPLE and ENERGY Code Mixing Models", DOE/ET/37240-78TR, July 1980.

* Revised - See Section B.2

B.1 Original Topical Reports (Continued)

J. T. Hawley, C. Chiu, W. M. Rohsenow, N. E. Todreas, "Correlations for Subchannel and Bundle Friction Factors and Flowsplit Parameters for Laminar, Transition, and Turbulent Longitudinal Flows in Wire Wrap Spaced Hexagonal Arrays", DOE/ET/37240-79TR, December 1980.

J. T. Hawley, C. Chiu, N. E. Todreas, "M.I.T. Extraction Method for Measuring Average Subchannel Axial Velocities in Reactor Assemblies", DOE/ET/37240-80TR, July 1980.

K. J. Burns, W. M. Rohsenow, N. E. Todreas, "Laminar/ Transition Sweeping Flow Mixing Model for Wire Wrapped LMFBR Assemblies", DOE/ET/37240-81TR, July 1980.

T.E. Greene, N. E. Todreas, "Criteria for Onset of Mixed Convection in Wire Wrap Spaced Hexagonal Arrays", Report DOE/ET/37240-82TR, To be issued.

D. R. Boyle and M. W. Golay, "Transient Effects in Turbulence Modelling", DOE/ET/37240-83TR, Feb. 1980.

P. D. Symolon and N. E. Todreas, "Fluid Mixing Studies in a Hexagonal 217 Pin Wire Wrapped Rod Bundle", DOE/ET/37240-84TR, Feb. 1981.

S. F. Wang, W. M. Rohsenow, and N. E. Todreas, "Flow Split, Pressure Drop, and Mixing Experiments in a 61 Pin Shaved-Wire Blanket Assembly, DOE/ET/37240-86TR, Feb. 1981.

S. F. Wang, N. E. Todreas, "Computer Model for M.I.T. Correlations for Friction Factors, Flow Split, and Mixing Parameters in LMFBR Wire-Wrapped Rod Assemblies, DOE/ET/37240-87TR, Feb. 1981.

S. F. Wang and N. E. Todreas, "Experimental Investigations of Laminar Mixed Convection in a Square Array of Bare Rods", Report No. DOE/ET/37240-88TR, Feb. 1981.

Reports Issued Under This Contract

B.2 Revised Topical Reports (Available from National Technical Information Service, U.S. Department of Commerce, Springfield, VA 22151)

S. F. Wang and N. E. Todreas, "Input Parameters to Codes Which Analyze LMFBR Wire-Wrapped Bundles," COO-2245-17TR, (Revision I), MIT, May, 1979.

** E. Khan, W. Rohsenow, A. Sonin, N. Todreas, "Manual for ENERGY Codes I, II, III Computer Programs", COO-2245-18TR, Revision I, MIT, July 1976.

** B. C. Chen and N. E. Todreas, "Prediction of Coolant Temperature Field in a Breeder Reactor Including Inter-assembly Heat Transfer," COO-2245-20TR, (Revision I), MIT, December, 1976.

H. Khan, "Fabrication Details for Wire-Wrapped Fuel Assembly Components," COO-2245-27TR, (Revision I), MIT, September, 1978.

** K. W. Chiu, "Fabrication Details for Wire-Wrapped Fuel Assembly Components," COO-2245-27TR, (Revision II), MIT, September, 1979.

C. Chiu, W. M. Rohsenow and N. E. Todreas, "Turbulent Sweeping Flow Mixing Model for Wire Wrapped LMFBR Assemblies", COO-2245-55TR, Rev. 1, MIT 1978.

** J. T. Hawley, Y. N. Chan and N. E. Todreas, "Input Parameters to Codes which Analyze LMFBR Wire Wrapped Bundles", COO-2245-17TR, (Revision II), December 1980.

** P. D. Symolon and N. E. Todreas, "Fluid Mixing Studies in a Hexagonal 61 Pin Wire Wrapped Rod Bundle", COO-2245-51TR, (Revision I), February 1981.

** Y. N. Chan and N. E. Todreas, "Turbulent Sweeping Flow Mixing Model for Wire Wrapped LMFBR Assemblies", COO-2245-55TR, (Revision II), December 1980.

** Y. N. Chan and N. E. Todreas, "Turbulent Flow Split Model and Supporting Experiments for Wire Wrapped Core Assemblies", COO-2245-56TR, (Revision I), December 1980.

** Y. N. Chan and N. E. Todreas, "Laboratory Manual for Salt Mixing Test in 37- and 217-Pin Bundles", COO-2245-62TR, (Revision I), August 1980.

** Latest Revision

Reports Issued Under This Contract

C. Papers and Summaries

Y. B. Chen, K. L. Ip, and N. E. Todreas, "Velocity Measurements in Edge Channels of Wire-Wrapped LMFBR Fuel Assemblies," American Nuclear Society Transactions, Vol. 19, 1974, pp. 323-324.

P. Carajilescov and N. Todreas, "Experimental and Analytical Study of Axial Turbulent Flows in an Interior Subchannel of a Bare Rod Bundle," J. of Heat Transfer, Vol. 98, No. 2, May 1976, pp. 262-268, (Included as Appendix to Quarterly Progress Report, COO-2245-15).

E. Khan, W. Rohsenow, A. Sonin, and N. Todreas, "A Porous Body Model for Predicting Temperature Distribution in Wire-Wrapped Fuel Rod Assemblies," Nuclear Engineering and Design, 35 (1975), pp. 1-12.

E. Khan, W. Rohsenow, A. Sonin, and N. Todreas, "A Porous Body Model for Predicting Temperature Distribution in Wire-Wrapped Rod Assemblies Operating in Combined Forced and Free Convection," Nuclear Engineering and Design, 35 (1975), pp. 199-211.

R. G. Bennett and M. W. Golay, "Development of An Optical Method for Measurement of Temperature Fluctuation in Turbulent Flows," American Nuclear Society Transactions, Vol. 22, 1975, p. 581.

B. Chen and N. Todreas, "Prediction of the Coolant Temperature Field in a Breeder Reactor Including Interassembly Heat Transfer," Nuclear Engineering and Design, 35, (1975), pp. 423-440, (Included as Appendix to Quarterly Progress Report, COO-2245-23).

R. Bennett and M. W. Golay, "Interferometric Investigation of Turbulently Fluctuating Temperature in an LMFBR Outlet Plenum Geometry," Presented at the ASME Annual Winter Meeting, December, 1976, (Included as Appendix in Quarterly Progress Report, COO-2245-30).

B. B. Mikic, E. U. Khan, and N. E. Todreas, "An Approximate Method for Predicting Temperature Distribution in Wire-Wrapped Fuel Assemblies of a Liquid Metal Fast Breeder Reactor," Mech. Res. Comm., Vol. 3, (1976), pp. 353-360.

L. Wolf, R. Karimi, J. Y. Kim, C. N. Wong, and M. K. Yeung, "2-D Thermoelastic Analysis of LMFBR Fuel Rod Claddings," Paper C4/d, 4th International Conf. Structural Mechanics in Reactor Technology, San Francisco, August 1977.

Reports Issued Under This Contract

C. Papers and Summaries (Continued)

M. Yeung, and L. Wolf, "Effective Conduction Mixing Lengths for Subchannel Analysis of Finite Hexagonal LMFBR Bundles," Transactions of the American Nuclear Society, June 1977, Vol. 26, pp 463-464.

C. Chiu and N. Todreas, "Flow Split Measurements in an LMFBR Radial Blanket Assembly," Transactions of the American Nuclear Society, June 1977, Vol. 26, pp 455-456.

J. Y. Kim and L. Wolf, "Laminar Mixed Convection Heat Transfer in Finite Hexagonal Bundles," Transactions of the American Nuclear Society, (1977), Vol. 27, pp 384-385.

J. Kelly and N. Todreas, "Turbulent Interchange in Triangular Array Bare Rod Bundles," Paper NR-3, Presented at Sixth International Heat Transfer Conference, Toronto, August 1978.

C. Chiu, N. E. Todreas, and W. M. Rohsenow, "Turbulent Flow Split Experiment and Model for Wire-Wrapped Assemblies," Transactions of the American Nuclear Society, June, 1978, Vol. 28, TANSAO 28, (1978), pp 536-537, ISSN: 0003-018X.

C. Chiu, N. E. Todreas, and W. M. Rohsenow, "Pressure Drop Measurements in LMFBR Wire-Wrapped Blanket Bundles," Transactions of the American Nuclear Society, Vol. 30, pp 541-543, (1978).

C. Chiu, N. E. Todreas, and W. M. Rohsenow, "Turbulent Mixing Experiment and Model for Wire-Wrapped Assemblies," Trans. of the American Nuclear Society, Vol. 30, pp 547-548 (1978).

M. Fakory and N. Todreas, "Experimental Investigation of Flow Resistance and Wall Shear Stress in the Interior Subchannel of a Triangular Array of Parallel Rods," Jl. Fluids Eng., Vol. 101, pp 429-435 (Dec. 1979).

J. G. Bartzis and N. E. Todreas, "Turbulence Modeling of Axial Flow in a Bare Rod Bundle," Jl. Ht. Trans., Vol. 101, No. 4, pp 628-634 (Nov. 1979).

C. Chiu, W. M. Rohsenow, and N. E. Todreas, "Turbulent Flow Split Model and Supporting Experiments for Wire-Wrapped Core Assemblies," Accepted for pub'n in Nuclear Technology.

Reports Issued Under This Contract

C. Papers and Summaries (Continued)

C. Chiu, W. M. Rohsenow, and N. E. Todreas, "Prediction of Temperature Distribution in Wire-Wrapped Nuclear Fuel Rod Assemblies," Proceedings NATO Mtg, Vol. 1, pp 175-184, published by Hemisphere Pub. Co., Washington, DC (1978).

S. Glazer, T. Greene, N. Todreas, and L. Wolf, "Transient Thermal-Hydraulic Analysis in the Forced-Convection Regime (TRANSENERGY)," TANSOA, Vol. 32, Atlanta, 1979.

C. Chiu, W. M. Rohsenow, and N. E. Todreas, "Turbulent Flow Split Model and Supporting Experiments for Wire-Wrapped Core Assemblies," Accepted for pub'n, Nuclear Technology, April 1980.

Chiu, C., Hawley, J. T., Rohsenow, W. M., and Todreas, N. E., "Parameters for Laminar, Transition and Turbulent Longitudinal Flows in Wire Wrap Spaced Hexagonal Arrays," Accepted for presentation at the Topical Meeting on Nuclear Reactor Thermal Hydraulics, Saratoga, NY, October 5-8, 1980.

Rohsenow, W. M., Todreas, N. E., Wang, S. F., "Buoyancy Effects on Subchannel Friction Factors in Bare Rod Bundles," Submitted for consideration at Specialists' Meeting on Decay Heat Removal and Natural Convection in FBRs," February 28-29, 1980, Upton, New York.

Chiu, C., Morris, R., and N. Todreas, "Experimental Techniques for Liquid Metal Cooled Fast Breeder Reactor Fuel Assembly Thermal/Hydraulic Tests," Invited Paper for Special Issue of Nuclear Engineering and Design ,Vol.62,No.1-3,pp 253-270,Dec.1980.

Bishop, A. and N. Todreas, "Hydraulic Characteristics of Wire-Wrapped Rod Bundles," Invited Paper for Special Issue of Nuclear Engineering and Design, Vol.62,No.1-3,pp 271-293,Dec.1980.

COOLANT MIXING IN LMFBR ROD BUNDLES AND OUTLET PLENUM MIXING TRANSIENTS

Contract AT(11-1)-2245

QUARTERLY PROGRESS REPORT

The work of this contract has been divided into the following Tasks:

TASK I: BUNDLE GEOMETRY (WRAPPED AND BARE RODS)

- TASK IA: Assessment of Available Data
- TASK IB: Experimental Bundle Water Mixing Investigation
- TASK IC: Experimental Bundle Peripheral Velocity Measurements (Laser Anemometer)
- TASK ID: Analytic Model Development - Bundles

TASK II: SUBCHANNEL GEOMETRY (BARE RODS)

- TASK IIA: Assessment of Available Data
- TASK IIB: Experimental Subchannel Water Mixing Investigation
- TASK IIC: Experimental Subchannel Local Parameter Measurements (Laser Anemometer)
- TASK IID: Analytic Model Development-Subchannels

TASK III: LMFBR OUTLET PLENUM FLOW MIXING

- TASK IIIA: Analytical and Experimental Investigation of Velocity and Temperature Fields

TASK IV: THEORETICAL DETERMINATION OF LOCAL TEMPERATURE FIELDS IN LMFBR FUEL ROD BUNDLES

TASK I: BUNDLE GEOMETRY (WRAPPED AND BARE RODS)

I.A Assessment of Available Data

I.B Experimental Bundle Water Investigations

I.B.1 61 Pin Fuel Bundles - Turbulent Flow
I.B.2 61 Pin Fuel Bundles - Laminar and Transition Flow
I.B.3 217 Pin Fuel Bundle
I.B.4 61 Pin Blanket Bundles
I.B.5 Shaved Wire 61 Pin Blanket Bundle
I.B.6 37 Pin (P/D=1.15) Bundle
I.B.7 Experimental Method for Flow Split Determination
I.B.8 Experimental Method for Pressure Drop Determination
I.B.9 Experimental Method for Mixing Parameter Determination

I.C Experimental Bundle Peripheral Velocity Measurements (Laser Anemometer)

I.D Analytic Model Development - Bundles

I.D.1 Steady State ENERGY/SUPERENERGY
I.D.2 Transient TRANSENERGY
I.D.3 Models for Forced Convection Analysis (Pressure Drop, Flow Split and Mixing)
I.D.4 Models for Mixed Convection

I.D.4.1 Models for Mixed Convection - Subchannel
I.D.4.2 Models for Mixed Convection - Assembly
I.D.4.3 Models for Mixed Convection - Core
I.D.4.4 Predictors of Inception of Mixed Convection

I.D.5 Determination of Shape Factors

TASK I. BUNDLE GEOMETRY (WRAPPED AND BARE RODS)

I.A Assessment of Available Data

This work was last reported in Progress Report COO-2245-72 dated September 1, 1979 - November 30, 1979. No work was done in the current period.

I.B. EXPERIMENTAL BUNDLE WATER INVESTIGATIONS

I.B.1 61 Pin Fuel Bundles - Turbulent Flow

(Paul Symolon)

Work on this task has been completed. The results are reported in Report No. COO-2245-51TR Revision 1, February 1981.

I.B.2 61 Pin Fuel Bundles - Laminar and Transition Flow

(Paul Symolon)

Work on this task has been completed. The results are reported in Report No. COO-2245-51TR Revision 1, February 1981.

I.B.3 217 Pin Fuel Bundle

(Paul Symolon)

Work on this task has been completed. The results appear in Report No. DOE/ET/37240-84TR.

I.B.4 61 Pin Blanket Bundles

Work on these bundles was completed and reported in a series of topical reports by C. Chiu which are listed under B.1 - Original Topical Reports, and under C.-Papers and Summaries.

I.B.5 Shaved Wire 61-Pin Blanket Assembly

(Song-Feng Wang)

Work on this task has been completed. The results appear in Report No. DOE/ET/37240-86TR.

I.B.6 37-Pin (P/D-1.15,H/D=13.5) Bundle

(Yee-Ning Chan)

New stainless steel rods and wires have been procured with which to construct a wire-wrapped assembly in an extruded, hexagonal housing originally used for a 217-pin bundle. The preparation of the fuel pins will

begin soon. New flow collectors, a salt solution injector and the injection rods are being fabricated.

I.B.7 Experimental Method for Flow Split Determination

Work on this task was completed and reported in Report No. DOE/ET/37240-80 TR which is listed under B.1 of this report.

I.B.8 Experimental Method for Pressure Drop Determination

This work was completed and reported in Report No. DOE/ET/37240-77 TR which is listed under B. 1 of this report.

I.B.9 Experimental Method for Mixing Parameter Determination

(Yee Ning Chan)

This task has been completed and will be issued shortly as Report No. COO-2245-62TR (Revision I).

I.C. EXPERIMENTAL BUNDLE PERIPHERAL VELOCITY MEASUREMENTS

(Laser Anemometer)

No work is being done on this task at the present time.

I.D. ANALYTICAL MODEL DEVELOPMENT - BUNDLES

I.D.1 Steady-State ENERGY-III

(Tom Greene)

No work was performed on this task during the present period; the last results on work in this area were reported in DOE/ET/37240-76.

I.D.2 Transient TRANSENERGY

(Tom Greene)

No work was performed in this area during the present period.

I.D.3 Models for Forced Convection Analysis

Pressure Drop and Flow Split Models

(Sang-Nyung Kim)

The latest versions of the flowsplit and friction factor correlations of laminar, turbulent, transition flow in wire-wrapped LMFBR rod bundle have been incorporated into the Computer Code ENERGY-III. These correlations are the work of J. Hawley and appear in Report No. DOE/ET/37240-79TR.

I.D.4 Models for Mixed Convection

(Paul Symolon)

During this quarter, work has continued on a literature survey of mixed convection in vertical tubes, and on vertical surfaces. The review is organized in the following fashion:

(1) Prandtl number effects in mixed convection
(2) Flow regime criteria
(3) Data and correlations
(4) Instability and transition to turbulence
(5) Discussion and conclusions

Due to an interruption of contract funding, no progress has been made on modification of the COBRA-WC Code to MULTICS Fortran. Work has been done on the design of the instrumented heater rod for the 4x4 rod test section. Details will be given when the design is finalized. Table 1 summarizes the important parameters in mixed convection found throughout the literature review. Refer to this table if any nomenclature is unclear.

PRANDTL NUMBER EFFECTS IN MIXED CONVECTION

Since the present research effort is directed toward LMFBR applications (low Prandtl number fluid) the determination of the effect of Prandtl number on mixed convection is of importance, particularly since much of the existing data is for water and air (moderate Prandtl number).

Lloyd and Sparrow [1] analytically determined velocity and temperature profiles for laminar mixed convection flow adjacent to a heated vertical flat plate using

the method of local similarity. Their results for dimensionless velocity and temperature profiles are given in Figure 1 for Pr = 100, .72, and .003. It can be seen that for a given Gr_x/Re_x^2, the distortion of the velocity and temperature profiles is much larger for the smaller Prandtl number flows. Similar results were obtained by Hommel [2] and Szewczyk [3].

A physical explanation for this behavior follows: The "velocity overshoot" near the wall, or type II profile observed for the lower Pr of Figure 1 is a result of buoyancy forces near the wall, which in turn is a result of the temperature profile. For a high Prandtl number, the thermal boundary layer is thin with respect to the momentum boundary layer, as exhibited in Figure 2. Within the momentum boundary layer, the dynamics of the flow are dominated by viscous effects.

The thermal boundary layer can be considered a region enclosing the buoyancy effects. Therefore, for high Prandtl number, all of the buoyancy effects lie in a region dominated by viscosity, so no velocity overshoot occurs (viscous forces balance buoyancy forces). For a low Prandtl number, the momentum boundary layer is thin, so much of the buoyancy effects lie in the inertia dominated region (see Figure 2). In this region, inertia forces balance buoyancy forces, and velocity overshoot can occur. The inertia force is proportional to

$u\frac{du}{dx}$ so large buoyancy forces in the outer region causes $u\frac{du}{dx}$ to be large, and overshoot occurs (small Pr), zero buoyancy force in the outer region causes $u\frac{du}{dx}$ to be zero, and no overshoot occurs.

The same argument may be applied to a developing internal flow, but the overshoot phenomena may be more dramatic, because any increase in velocity near the wall will be accompanied by a decrease in the centerline velocity, due to mass conservation.

Figure 3 gives some of the experimental results of Buhr, et al [4] who measured velocity and temperature profiles, along with Nusselt numbers at a fixed axial location ($\frac{z}{d} = 74$) in a vertical pipe with turbulent flow of mercury. The velocity profiles of Figures 3a, 3b and 3c show the effect of varying the heat flux ($\frac{R_a}{R_e}$) at Reynolds numbers of approximately 20,000, 30,000 and 60,000. As the heat flux is increased the velocity profile distorts with the velocity increasing near the wall, and decreasing at the centerline. Figure 3d shows how the Nusselt number varies with heat flux for the three Reynolds numbers ($R_e = P_e/P_r$). Note that for all three cases the Nusselt number minima corresponds to the flattest velocity profile, which occurs at $\frac{R_a}{R_e} = 0.4$ to 0.6. This observation is in agreement with the argument in the previous progress report regarding a decrease in the turbulence production for flat

velocity profiles. Buhr also observed that for high heat fluxes, limiting velocity and temperature profiles are obtained.

Buoyancy-induced laminarization has also been observed in mixed convection flow of sodium by Wendling, et al [5]. Laminarization is predicted by Petukhov and Zhilin [6] for the flow of liquid metals in magnetic fields. In this case, it is the magnetic forces rather than the buoyancy forces which reduce the turbulence production.

FLOW REGIME IDENTIFICATION AND CRITERIA

Since buoyancy plays an important role in many practical heat transfer calculations, it is important to know when the buoyant flow can be neglected with respect to the forced flow (forced convection regime); when the forced flow can be neglected with respect to the buoyancy flow (free convection regime); and when both are important (mixed convection regime). In each of the above cases, it is also of interest to determine if the flow is laminar or turbulent. The flow regime map of Metais and Eckert [7] given in Figure 4 allows these regimes to be identified for flow through vertical tubes based on the parameters R_e and $G_r P_r (\frac{D}{L})$ for $10^{-2} < P_r < 1$.

Additional criteria for mixed convection are presented in Table 1. The criteria of Jackson and Hall [8] was derived by expressing the fractional reduction in shear stress due to buoyancy at $y^+=30$ in terms of fluid properties and flow properties (Re and C_f). the effect of the shear

stress on heat transfer was estimated, and C_f was expressed as $.046\ R_e^{-.2}$ to give the criteria shown. The criteria is difficult to apply, because the wall temperature must be known to evaluate the Grashof number.

The criteria of Polyakov [9] was derived by working with the turbulent energy equation, keeping the generation, dissipation, and buoyancy terms. He derived equations for friction factor and Nusselt number under mixed convection conditions when the influence of buoyancy is small. From these equations he derived the two criteria given in Table 1. His results show that for smaller P_r, the influence of buoyancy appears earlier.

Kenning, et al [10] experimentally determined a criteria for when wall temperature peaking occurs. This regime can be considered a subset of the mixed convection regime.

Hall [11] derived a criteria for when heat transfer is significantly impaired by buoyancy by deriving an expression for when the shear stress at $Y^+ = 30$ is approximately zero, and hence the turbulence production nearly zero.

DATA AND CORRELATIONS

Figure 5 shows the flow regime criteria of Alferov et al [17]. Figs. a-d correspond to pipe diameters of 30mm, 20mm, 14mm, and 8mm respectively. For given heat flux (q), and mean bulk temperature (t_l) a point can be located on the

plot. If the point lies above the boundary line for the particular mass velocity, buoyancy forces must be considered.

Figure 6 presents the correlations of Petukhov and Strigin [12,13] along with figures showing the general trends predicted.

Figure 7 gives the data and correlations of Kenning, et al [10]. Peaking in wall temperature was observed for higher heat fluxes, and was attributed to a reduction in turbulence production due to large buoyancy forces. The subsequent recovery occurred when the wall layer moved faster than the fluid in the core (Type II profile, or "Thermal Plume" in BNWL literature).

Some of the results of Connor and Carr [14] for the aiding flow of air in a vertical tube are given in Figure 8. Curves 1-4 show the effect of increasing the heat flux on velocity, turbulent shear stress, and turbulent velocity intensity profiles. The Nusselt numbers corresponding to profiles 1-4 are 14.8, 9.8, 10.6, and 10.7, respectively. The minimum Nusselt number corresponds to the flat velocity profile (#2) and the nearly zero shear stress profile. The improvement in heat transfer results when the Type II profile develops, and the turbulent shear stress near the wall (and hence the turbulence production) starts to increase. The minimum heat transfer corresponds also to a minimum turbulent intensity profile. Note that the turbulent velocity intensity distribution for profile #2 is minimum at $Y/R = 1.0$, but not a $Y/R = .2$, which is contrary to my expectation.

Figure 9 summarizes some of the results of Byrne and Ejiogu [16] for air flow in a vertical pipe. Fig. 8a shows the effect of Grashof number on a Nu vs Re plot. For higher Gr, a minima occurs in the Nusselt number due to laminarization. Figure 8b shows the same data with a plot of constant Nu on a Gr-Re plane. It also shows that the minima in heat transfer corresponds closely to their criteria (see Table 2). Their criteria for buoyancy forces having some effect appears to be quite conservative. The turbulence intensity and velocity profiles across the tube are given in Figures 8c and 8d respectively. Note that for the $Gr = 1.34 \times 10^9$ run of Figure 8a the minimum Nu occurs at $Re \cong 4 \times 10^4$, which also corresponds with the minima in turbulence intensity of Figure 8c, and the flat velocity profile of Figure 8d. This is in agreement with the turbulence production argument of the previous Progress Report.

Some of the results of Alferov, et al [17] are presented in Figure 10. The first plot shows the wall temperature distribution for both upflow and downflow of water, and the second plot shows the corresponding heat transfer coefficients ($\alpha_t/\alpha_f = Nu/Nu_T$) for a typical run. Note that for downflow, α_t/α_f is constant with x/d, but for upflow, local deterioration in heat transfer is observed due to laminarization. This is followed by a region of stabilized (fully-developed) heat transfer. The final

plot shows a best-fit of the Nusselt number data plotted against Ra_A/Re^2. Curve "a" is plot of the minimum Nusselt number (α_{MIN}/α_f which occurs at $(x/d)_{MIN}$), curve "b" is a plot of the fully developed Nusselt number (α_{st}/α_f which occurs for $(x/d) > (x/d)_{ST}$), and curve "c" is the Nusselt number for downflow.

This plot displays vividly the three regimes of heat transfer:

(1) When $Ra_A/Re^2 < 3 \cdot 10^{-6}$, the three curves converge into one where $\alpha/\alpha_f = 1$. This is the forced convection regime, where the heat transfer depends on Re only.

(2) When $Ra_A/Re^2 < 1$, the three curves converge into one which is Reynolds number independent. This is the natural convection regime.

(3) When $\frac{Ra_A}{Re^2} = 3 \times 10^{-6}$ to 1, both Re and Ra_A are important in determining heat transfer. This is the mixed convection regime.

Correlations were also presented for the distance to the heat transfer minima $(x/d)_{MIN}$, and the distance to developed heat transfer $(x/d)_{st}$.

INSTABILITY AND TRANSITION TO TURBULENCE

Since the heat transfer and frictional characteristics of a turbulent flow are considerably different from that of a laminar flow, it is important to accurately predict the transition from laminar to turbulent flow. Mathematically, this prediction boils down to the following

question: Can a given laminar flow withstand a disturbance and still return to its original state? If so, it is stable and the laminar flow will remain. If not, a transition to turbulence will eventually occur.

The analytical tool used to investigate this question is linear stability theory. First, it is assumed that there is a known solution Q_o to the governing differential equation. Then a disturbance Q' is introduced into the equation. The terms in Q_o can be subtracted out since it identically satisfies the equation. What remains is the disturbance equation for Q', which is a nonlinear partial, differential equation. If Q' is assumed small, and products and powers of disturbance variables are neglected, a set of linear partial differential equations are obtained. Further simplification results if the flow is assumed to depend on only one space coordinate (parallel flow assumption). For a given disturbance frequency the equations can be solved for the neutral curves, which form a boundary for the stable and unstable regions.

For a forced flow, the resulting equations (known as the Orr-Sommerfeld equations) are of fourth order, but when buoyancy forces are accounted for they are of sixth order. Their complexity has left them unsolved until the development of high capacity machines and sophisticated numerical techniques. If viscosity is neglected, somewhat

simpler second order equations result. For this case it can be shown [18] that a necessary condition for instability is that the velocity profile has a point of inflection. This is known as the "inviscid instability".

Gebhart [19] studied the stability of a natural convection flow over a vertical flat plate. He calculated the neutral stability curves allowing for the effect of wall heat capacity.

Stability theory tells us that the critical Reynolds number depends only on the velocity profile shape. Many investigators replace stability analysis with experiment plus a laminar flow computer solution, and correlate instability with a particular profile shape calculated by the code. Some examples of this follow:

Scheele and Hanratty [20] investigated experimentally the stability of fully developed mixed convection flow in a vertical pipe 762 diameters long. They found that stability depends primarily on the shape of the velocity profile, which in turn depends on the power to flow ratio (Gr/Re). For aiding flow, instability occurs when the velocity profile develops points of inflection, and transition to turbulence involves the gradual groth of small disturbances. For opposing flow instability is associated with separation at the wall. Transition to turbulence occurred shortly thereafter. Figure 11 shows the velocity distributions for aiding and opposing flow. For aiding flow the

inflection point at the tube centerline occurs at Gr/Re= 32.94, and moves toward the wall for increasing Gr. At Gr/Re=319.1, the velocity at the centerline is zero and further increases in heat flux will cause reverse flow near the tube center. For opposing flow an inflection point at the wall occurs at Gr/Re=9.87, and moves toward the tube center for increasing Gr/Re. For Gr/Re =52.2, the velocity gradient at the wall is zero and further increases in Gr/Re result in reverse flow near the wall. These results infer that an inflection point at the wall is not as destabilizing as an inflection point at the centerline.

Sherwin and Wallis (21) studied developing laminar aiding flow in a heated vertical annulus. Figures 12a and 12b show their developing axial and radial profiles for $Gr_q/Re=400$ (the inner rod was heated, and the outer duct insulated). For $x \approx 3$ the velocity gradient at the outer surface was nearly zero. The magnitude of the radial velocities decreases with x until x=2.9, above which it increases. This behavior near x=3 was associated with the initiation of unstable flow. Figure 12c shows the numerical analysis of onset of flow instabilities along with their experimental results. Agreement is reasonable, and differences were attributed to asymmetry in the flow near the unstable region. This asymmetry was also observed by Scheele and Hanratty (20).

Lawrence (22) investigated laminar developing flow in a circular tube. His theoretical solution was used to obtain developing axial velocity profiles for the cases shown in Figure 13. The experimental data gave the axial position at which instability began. Thus calculated, unstable profiles were obtained for different Reynolds numbers. His results showed that transition always occurred after the profile had developed an inflection point with a Type II profile. This corresponds to the results of Scheele and Hanratty. By trial and error, Lawrence found a transition parameter based on the velocity profile shape, and correlated it against entrance Reynolds number as shown in Figure 14.

DISCUSSION AND CONCLUSIONS

The Nusselt number data of Buhr et al (4) for mercury was plotted as Nu versus Ra/Re, and a family of curves was obtained for each Pe (Figure 3d). If we replot this data using the correlating parameters of Petukhov and Strigin (12), the data correlates to within $\pm$ 10%, as shown in Figure 11. The Nusselt number minima occurs at $Ra/Re^2 \simeq 2\times10^{-5}$ and is 68% of the turbulent forced convection Nusselt number (given by the Lyon equation, $Nu=7+.025Pe^{.8}$). For comparison,

Petukhov's correlation for water data is drawn in. For water ($2<Pr<6$) the Nusselt number minima occurs at $Ra/Re^2 = 1.6\times10^{-3}$ and is 46% of the turbulent forced convection Nusselt number. From these results we can conclude that:

1) For a lower Pr fluid, the mixed convection regime is entered sooner (lower heat flux, higher Reynolds number) than for a higher Pr fluid. And,

2) The resulting deterioration in heat transfer is larger for the higher Pr fluid. Conclusion No. 1 follows from our discussion of Figure 2, and conclusion No. 2 may be expected because when buoyancy effects decrease the turbulent transfer, the higher molecular conductivity of a lower Pr fluid can sustain higher heat transfer rates due to conduction.

Table 3 gives estimated LMFBR normal and shutdown operating conditions. The geometry, linear power, and coolant velocity was taken from Reference 15. Fluid properties were evaluated at 900°F. The value of Ra/Re^2 for interior and edge subchannels for the fuel and blanket assembly is given. These results can be compared with Figure 11, which gives Nusselt number versus Ra/Re^2 for water ($Pr\simeq6$) and mercury ($Pr\simeq.02$).

Sodium has a Prandtl number less than that of mercury (Pr≈.005) so its curve is expected to lie to the left of the murcury curve. The Ra/Re^2 values of Table 3 show that an LMFBR in shutdown conditions is operating in the mixed convection regime. Furthermore, the edge channel of the blanket assembly can be expected to be in the "thermal plume" regime where heat transfer is enhanced by low Reynolds number turbulence and Type II velocity profiles near the heated wall.

Petukhov (13) has stated that his correlation is valid for $x/d>40$ where the flow and heat transfer are fully developed; hence he takes no account of the axial coordinate in his correlation. Kenning's results (10) show that the heat transfer coefficient is varying with x up to $x/d=80$, so it is doubtful that fully developed conditions are achieved for $x/d>40$ as stated by Petukhov.

It is apparent from Figure 15 that the parameter Ra/Re^2 does not correlate data for different Prandtl numbers. Connor and Carr (14) attempted to correlate data for various Prandtl number fluids in terms of the parameter Gr_A/Re^2. They found that the Type II flow data (data to right of Nusselt number minima in Fig. 15 where the maximum velocity is not at the tube centerline,

or the "Thermal Plume" flow regime from BNWL literature) is correlated by:

$$\frac{Nu}{Nu_T} = 8.84 \left| \frac{Gr_A}{Re^2} \right|^{.263} \qquad (1)$$

A plot of the Type II flow data and the correlation (equation 1) is given in Figure 16a The Type I flow data (velocity maximum occurring at the tube centerline) does not correlate in terms of this parameter.

As in Petukhov's correlation, an L/D factor is not included. Connor investigated the size of the errors introduced by not including an L/D factor by comparing the measurements of Kenning et al (10) at different axial locations with equation 1. This is done in Figure 16b where Type II flow data from five of Kenning's runs are shown. The chains of points represent measurements at different axial locations for the same run. Considerable variation is observed, but is generally less than 20% of the predicted value.

Though the Metais-Eckert flow regime map is not valid for low Prandtl number fluids, it is of interest to determine where the low Pr mixed convection regime lies on this plot. The parameter $GrPr \frac{D}{L}$ was calculated for each of Buhr's 20 runs. The points are plotted on the

flow regime map of Figure 17. Each chain of points represents a constant Reynolds number with the heat flux varied. The diagonal line $\overline{AA}$ represents those runs with flat velocity profiles (Runs 7, 12, and 15 from Figure 3). All of the points shown are in the turbulent mixed convection regime, but on the plot appear in the turbulent forced convection regime. The circled point (Run #16) is close to the forced convection regime, because $Nu/Nu_T=.88$ (the transition from the forced convection to the mixed convection regime is defined as the line where $Nu/Nu_T=.9$ by Metais and Eckert). Line $\overline{BB}$ must be close to the forced-mixed transition for low Pr fluids. The "Thermal Plume" regime for low Pr fluids is to the right of line $\overline{AA}$. In this region heat transfer is described accurately by equation 1, and Type II velocity profiles exist.

It appears to the author that the flow regime map gives the wrong Prandtl number effect. As discussed previously, the mixed convection regime is entered sooner for low Pr fluid than for a high Pr fluid. The flow regime map appears to give the opposite trend.

In this literature review, two experimental techniques have been discussed to investigate heat transfer in mixed convection flows. The first is to make

Measurements at a fixed axial location, and observe how things vary with heat flux and flow rate. Buhr and Petukhov used this technique. The second is to make measurements at various axial locations for a range of heat fluxes and flow rates. This technique was used by Kenning. Only with this technique can wall temperature peaking be observed. How then is wall temperature peaking related to the minima in the Nusselt number observed by Buhr and Petukhov? The answer is that the laminarization phenomena is occurring for each case, but how the velocity profile changes are brought about differs. What is important is the integrated heat addition from the inlet to the measuring plane. In one case the total heat added to the buoyant layer is varied by changing the heat flux, and for the other case it is varied by changing the measuring station.

Consider the Re=7,000 run of Kenning's data (Figure 6). For low heat fluxes h decreases with x. And T_w increases with x. Only for intermediate heat fluxes does h have a minimum. The data from this run has been transformed into the coordinates of Figure 11 with h/h_T plotted against q" for three x/d values. Figure 12 is an idealized plot with the noise in the data eliminated. These plots show:

1) If x/d effects are ignored when they are really present, larger scatter in the data will be observed (see also Figure 9b which shows same information) and wall temperature peaking will not be seen.

2) If x/d effects are considered, three regimes can be identified as shown on the plot. The wall temperature peaking regime can be identified where h initially decreases with x, then increases.

References

1. Lloyd and Sparrow, "Combined Forced and Free Convection Flow on Vertical Surfaces", IJHMT, 1970.

2. M. J. Hommel, "Mixed Convection Heat Transfer from a Vertical Plate: Prandtl Number Effects", ASME Paper 76-WA/HT-17,

3. A. A. Szewczyk, "Combined Free and Forced Convection Laminar Flow", JHT, November 1964.

4. Buhr, Horsten, and Carr, "The Distortion of Turbulent Velocity and Temperature Profiles on Heating for Murcury in a Vertical Pipe", JHT, May 1974.

5. Wendling, Ricque, and Martin, "Mixed Convection with Sodium", Progress in Heat and Mass Transfer, Dwyer, Vol. 7, 1973.

6. Petukhov and Zhilin, "Heat Transfer in Turbulent Flow of Liquid Metals in a Magnetic Field", Progress in Heat and Mass Transfer, Dwyer, Vol. 7, 1973.

7. Metias and Eckert, "Forced, Mixed, and Free Convection Regimes", JHT, May 1964.

8. Jackson and Hall, "Influences of Buoyancy on Heat Transfer to Fluids Flowing in Vertical Tubes under Turbulent Conditions", TURBULENT FORCED CONVECTION IN CHANNELS AND BUNDLES, 1979.

9. Polyakov, Transient Effects due to Thermogravity in Turbulence and Heat Transfer", HIGH TEMPERATURES Vol. 11, 1973.

10. Kenning, Shock and Poon, "Local Reductions in Heat Transfer due to Buoyancy Effects in Upward Turbulent Flow", 5th International Heat Transfer Conference, Tokyo, 1974.

11. Hall, "Heat Transfer Near the Critical Point", ADVANCES IN HEAT TRANSFER, Vol. 7

12. Petukhov and Strigin, "Experimental Investigation of Heat Transfer with Viscous-Inertial-Gravitational Flow of a Liquid in Vertical Tubes", HIGH TEMPERATURES, Vol. 6, 1968.

13. Petukhov, "Turbulent Flow and Heat Transfer in Pipes under Considerable Effect of Thermogravitational Forces", HEAT TRANSFER AND TURBULENT BUOYANT CONVECTION, 1977.

14. Connor and Car, "Heat Transfer in Vertical Tubes under Conditions of Mixed Free and Forced Convection", 6th International Heat Transfer Conference, Toronto, 1978.

15. S. F. Wang, "Natural Convection Effects in Isolated and Interconnecting Subchannels of a Reactor Fuel Assembly", Ph.D. Thesis, MIT, January 1981.

16. Byrne and Ejidgu, "Combined Free and Forced Convection Heat Transfer in a Vertical Pipe", HEAT AND MASS TRANSFER BY COMBINED FORCED AND NATURAL CONVECTION, 1971.

17. Alferov, Balunov, and Rybin, "Calculating Heat Transfer with Mixed Convection", Teploenergetika 1975 22(6).

18. H. Schlichting, BOUNDARY LAYER THEORY, McGraw Hill, 1969.

19. B. Gebhart, "Natural Convection Flow, Instability, and Transition", J. Ht. Transfer, August 1969.

20. Scheele and Hanratty, "Effect of Natural Convection on Stability of Flow in a Vertical Pipe:, J.F.M.,1962.

21. Sherwin and Wallis, "Combined Natural and Forced Laminar Convection for Upflow Through Heated Vertical Annuli", HEAT AND MASS TRANSFER BY COMBINED FORCED AND NATURAL CONVECTION, 1971.

22. W. T. Lawrence, "Entrance Flow and Transition from Laminar to Turbulent Flow in Vertical Tubes with Combined Free and Forced Convection", Sc. D. Thesis, mit, February 1965.

TABLE 1

Definitions of Important Dimensionless Parameters in Mixed Convection

Name	Dimensionless Group
Reynolds Number	$Re = \frac{Ud}{\nu}$
Rayleigh Number	$Ra = Gr\ Pr$
Prandtl Number	$Pr = \frac{C_p \mu}{K}$
Grashov Number (Basic Form)	$Gr = \frac{\beta g (T_w - T_b) d^3}{K \nu^2}$
Grashov Number Based on axial temperature gradient	$Gr_A = \frac{\beta g d^4}{\nu^2} (\frac{dT_b}{dx})$
	$= \frac{4\ GrNu}{Re\ Pr}$
	$= \frac{\beta g}{\rho \nu^2} \frac{d^4}{A_{xs}} \frac{q'}{U}$ (I.C.)
Grashov Number Based on heat flux	$Gr_q = \frac{g \beta q'' d^4}{K \nu^2}$
	$= Gr\ Nu$
Grashov Number Based on axial distance	$Gr_x = \frac{\beta g q'' x^4}{K \nu^2}$
	$= \frac{x^4}{d^4} Gr\ Nu$
Petukhov's Correlating Parameter	$\frac{Ra_A}{Re^2} = \frac{4\ GrNu}{Re^3}$
	$= \frac{d^2}{A_{xs}} \frac{g \beta \nu}{K} \frac{q'}{U^3}$ (I.C.)
Carr's Correlating Parameter	$\frac{Gr_A}{Re^2} = \frac{4\ GrNu}{Re^3 Pr}$
	$= \frac{d^2}{A_{xs}} \frac{g \beta}{\rho C_p} \frac{q'}{U^3}$ (I.C.)

IC=isolated cell only, i.e. $A = dT_b/dx = q'/\rho U A_{xs} C_p$

TABLE 2
CRITERIA FOR TURBULENT MIXED CONVECTION
FOR AIDING FLOW IN VERTICAL CIRCULAR TUBES

Author(s) (Reference)	Criteria	Equation	Range of Applicability
Jackson and Hall [8]	Criteria for when buoyancy reduces heat transfer coefficient from forced convection value by less than 5%.	$\frac{\bar{G}_r \left(\frac{\mu_w}{\mu_b}\right) \left(\frac{\rho_b}{\rho_w}\right)^{1/2}}{Re_b^{2.7} \, Pr_b^{5}} < 10^{-5}$	$.7 < Pr_b < 5$
Polyakov [9]	For when a 1% deviation of Nu from its forced convection value occurs	$Gr_q = \frac{1.3 \times 10^{-4} \, Re^{2.75} \, Pr \left[Re^{1/8} + 2.4 (Pr-1)\right]^{2/3}}{\log Re + 1.15 \log (5Pr+1) + \frac{1}{2} Pr - 1.8}$	$Pr \gtrsim 1$
	For when a 1% deviation of friction factor from forced convection occurs	$Gr_q = 2 \times 10^{-4} \, Pr \, Re^{2.75}$	
Kenning, et al [10]	For when wall temperature peaks (local reductions in heat transfer coefficient) occur	$\frac{Gr_b^*}{Re_b^{3.4} Pr_b^{4}} > 4 \times 10^{-5}$	$0 < x/d < 80$ $1.5 < Pr_b < 7$
Hall [11]	For when heat transfer is impaired by buoyancy	$\frac{G_r}{Re^{2.7}} \cong .7 \times 10^{-4}$	None given
Byrne and Ejiogu [16]	Criteria for significant buoyancy effect on heat transfer	$Gr/Re^{1.8} \cong .05$	None given
	For minimum heat transfer	$Gr/Re^{2.8} \cong 10^{-4}$	

TABLE 3

LMFBR Normal and Shutdown
Operating Conditions

Geometry		Fuel Assembly		Blanket Assembly	
Rod Diameter, ft		.0191666		.043333	
Hydraulic Diameter, ft	int.	.0138558		.0120904	
	edge	.01902166		.0187963	
Wetted Perimeter, ft	int.	.0301066		.0680666	
	edge	.0420858		.0914016	
Condition		Normal	Shutdown	Normal	Shutdown
Linear Power, kw/ft		~16	~.512	5.4~16	.248~.736
Coolant Velocity, ft/sec		25	.925	1.6~8	.059~.296
Power-to-Flow Ratio*		1.0	.865	1.0	1.243
Re	int.	1.1E5	4084	3.5-17 E4	227 - 6412
	edge	1.5E5	5605	.96-4.7E4	353 - 1772
Ra	int.	32.3	28.2	18.6 - 65	37 - 128
	edge	60.1	52.4	52 - 182	102 - 359
Ra/Re^2	int.	2.6E-9	1.7E-6	.15-2.2 E-9	.007-3.1 E-6
	edge	2.7E-9	1.7E-6	.56-8.2 E-8	1.1-8.2 E-4

FIGURE 1

Analytical results of Lloyd and Sparrow (1)

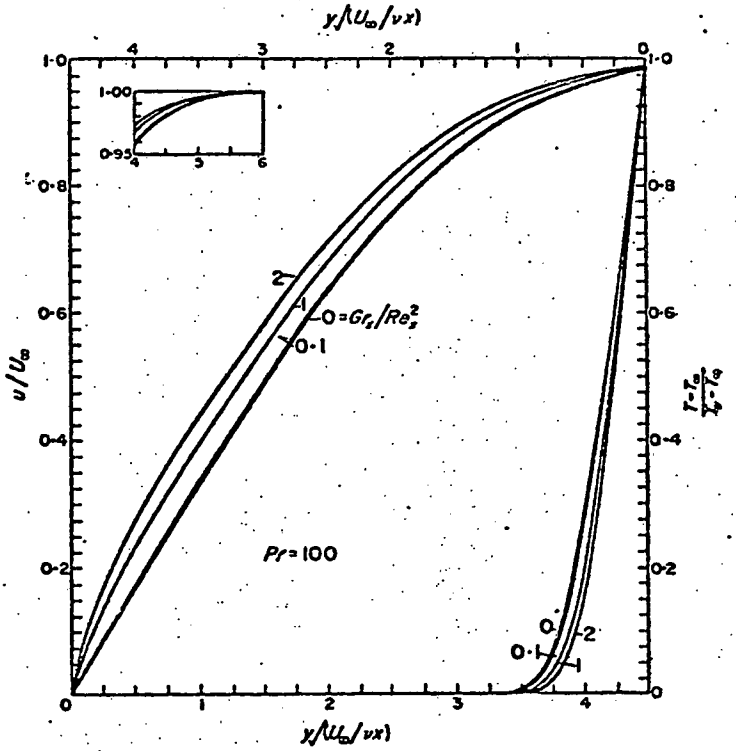

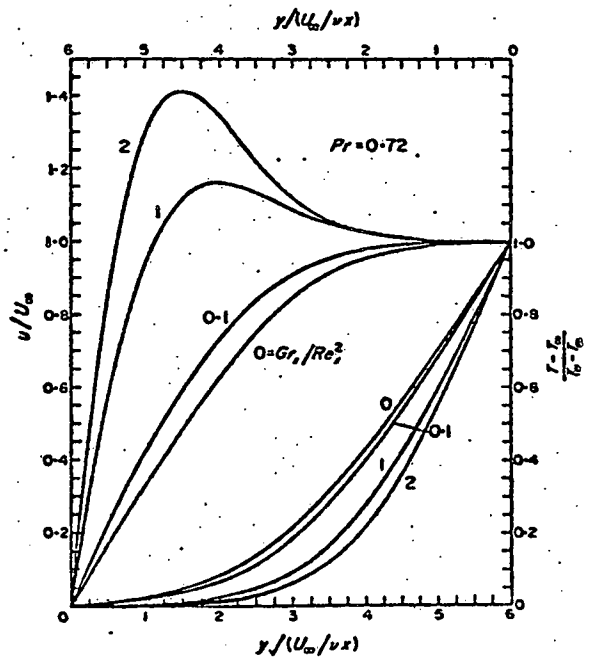

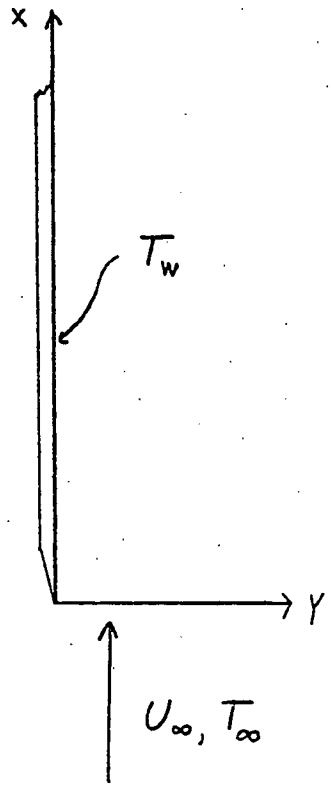

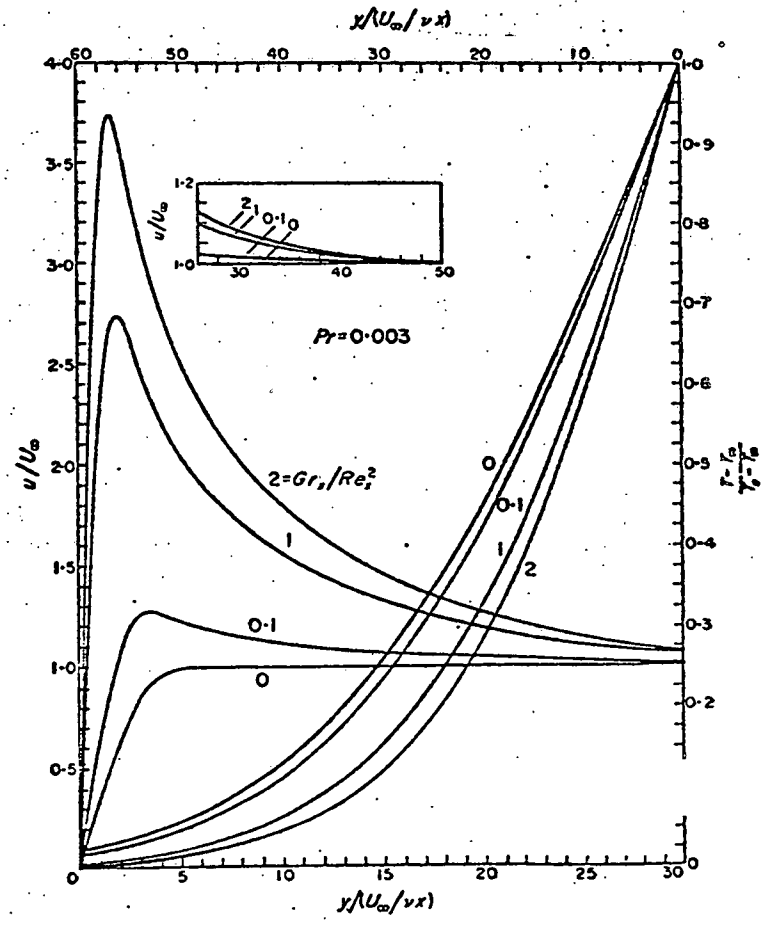

FIGURE 2

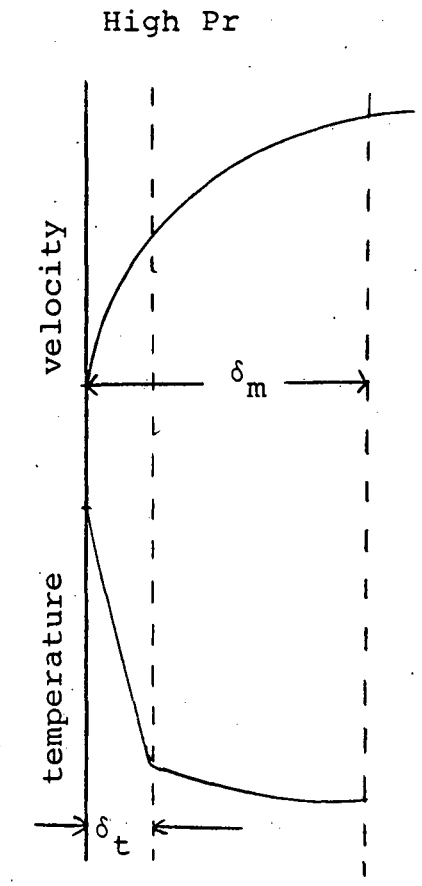
High Pr
velocity
δ_m
temperature
δ_t

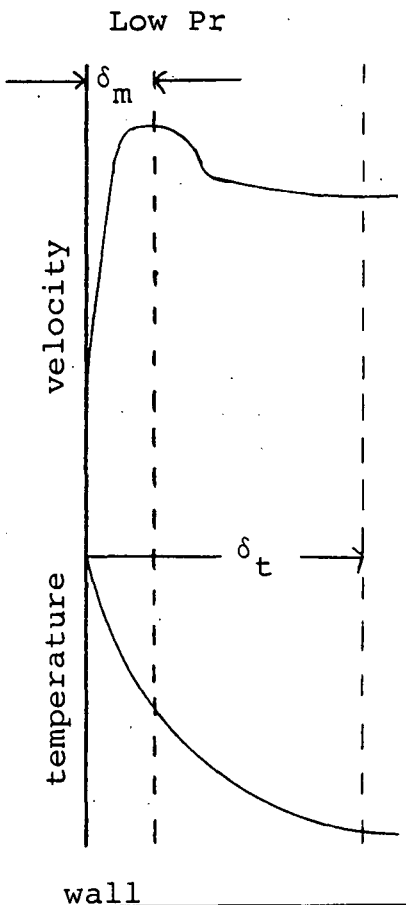
Low Pr
δ_m
velocity
δ_t
temperature
wall

FIGURE 3

Experimental Results of Buhr et al (4)

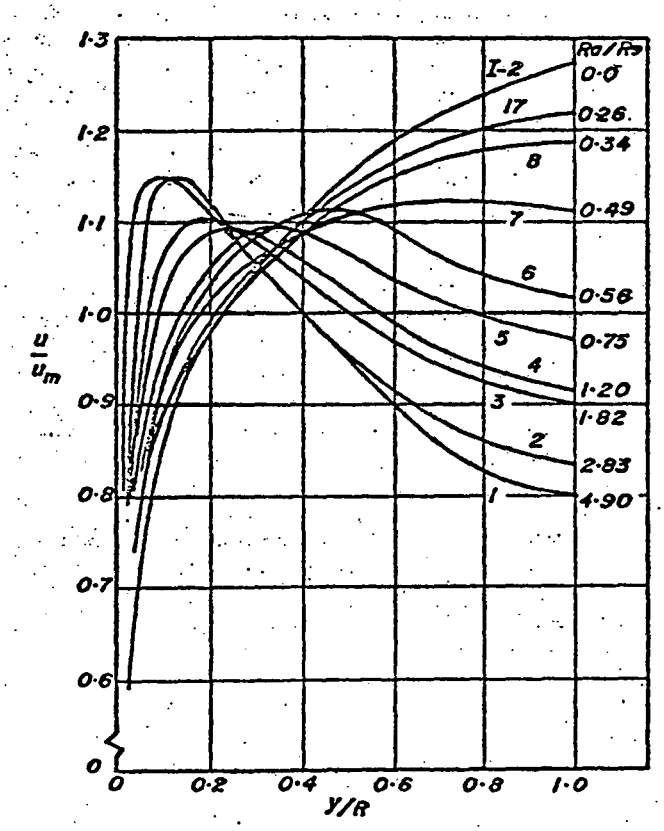

Fig. 3(a)

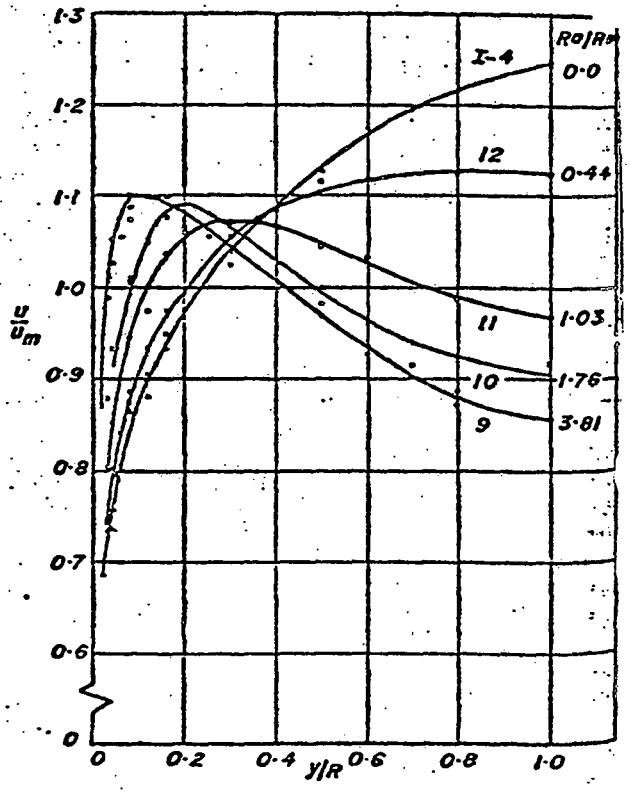

Fig. 3(b)

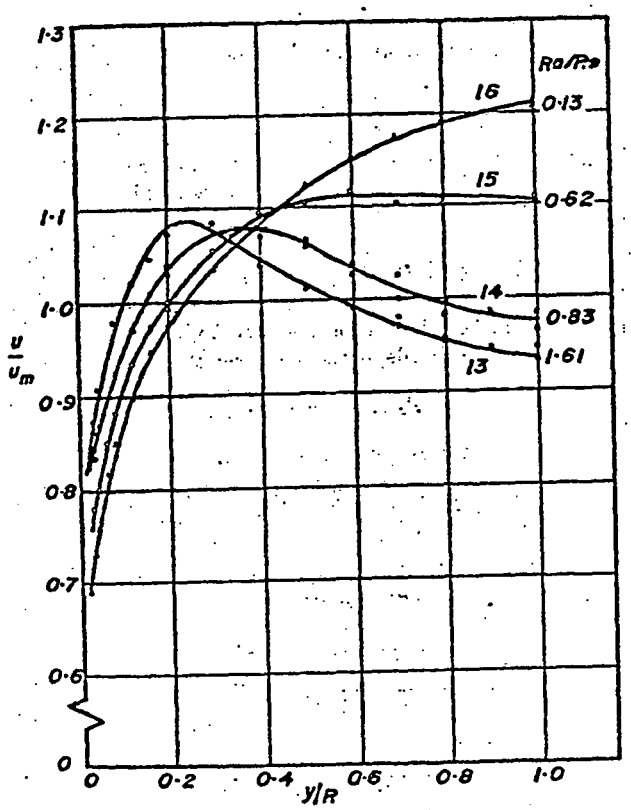

Fig. 3(c)

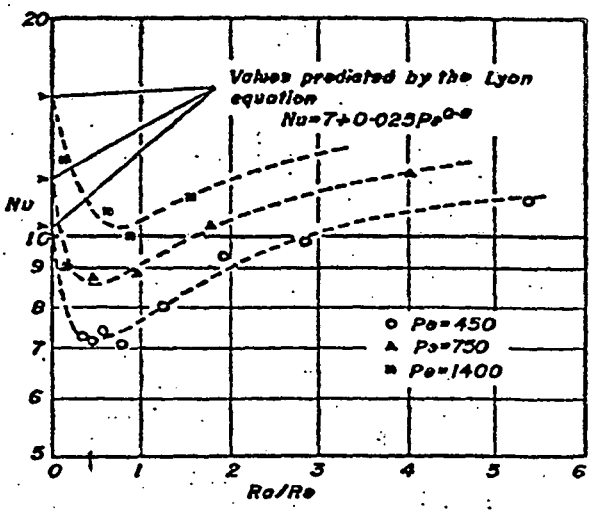

Fig. 4 Variation of Nusselt number with heat flux

FIGURE 4

Flow regime map for flow in vertical tubes (Metais and Eckert (7))

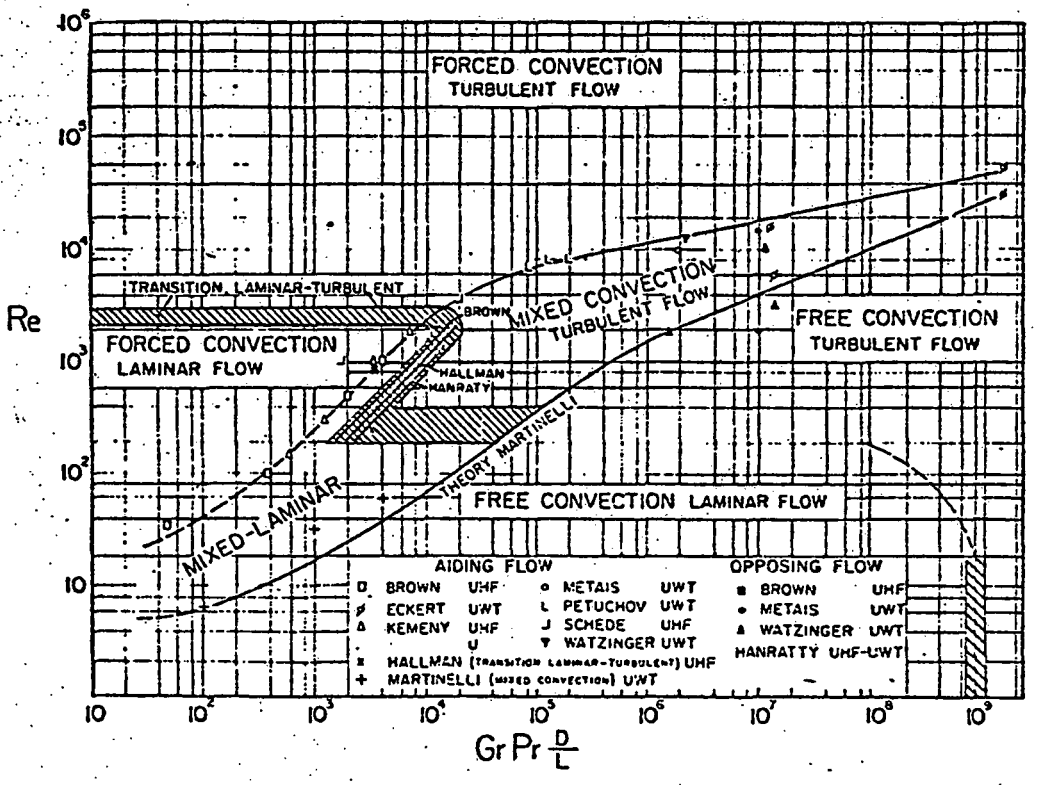

Regimes of free, forced, and mixed convection for flow through vertical tubes

$$\left(10^{-2} < Pr\,\frac{d}{L} < 1\right)$$

FIGURE 5

Flow regime map of Alferov et al (17)

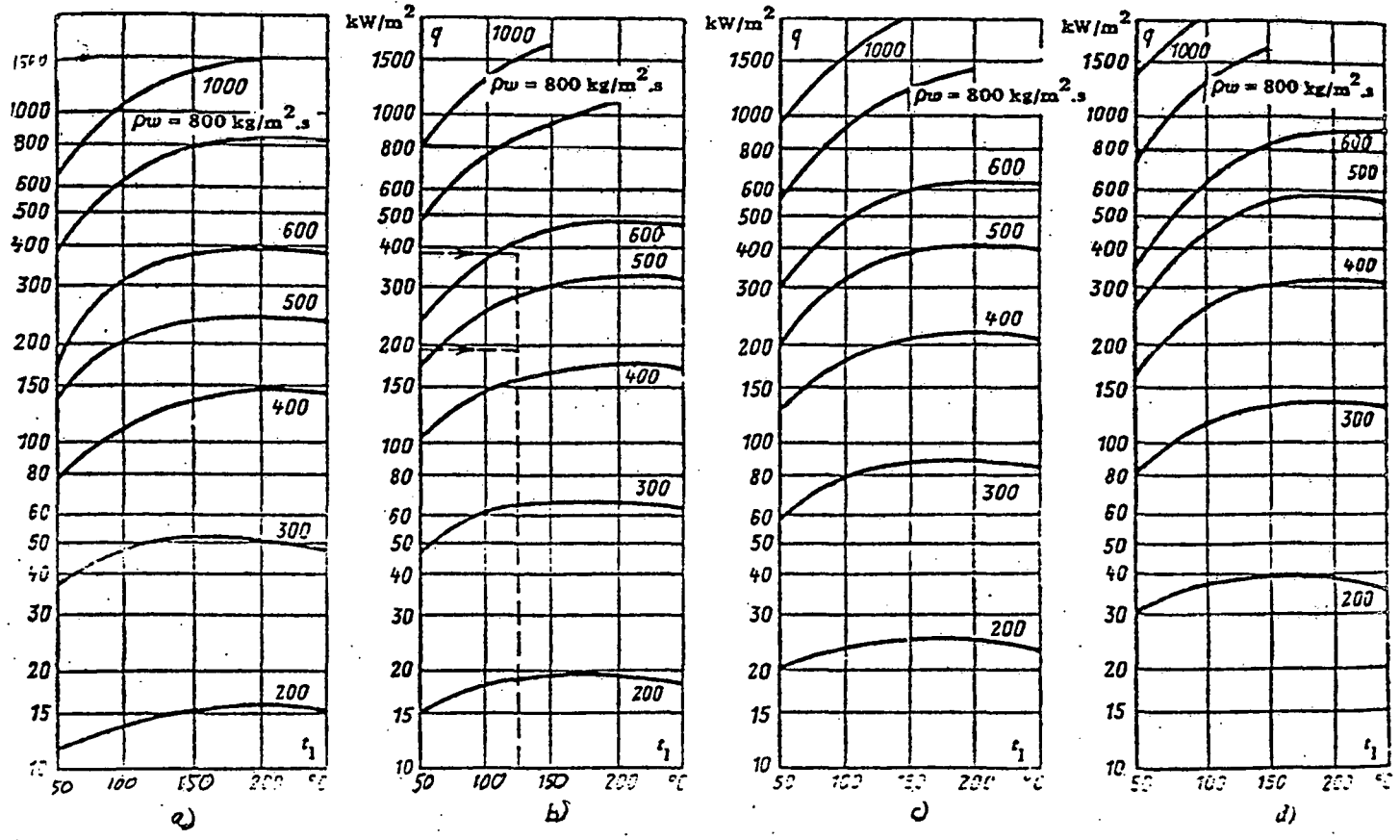

FIGURE 6

Correlations of Petukhov and Strigin (12,13)

Correlation	Range of Validity
$\frac{Nu}{Nu_o} = [1+720\ \frac{Ra}{Re}]^{-1}$	$\frac{Ra}{Re} < 1.6\times10^{-3}$ $2< Pr< 6$ $x/d>40$
$\frac{Nu}{Nu_o} = 3.97(\frac{Ra}{Re})^{1/3}$	$16 < \frac{Ra}{Re} < 1.6\times10^{-3}$ $2< Pr< 6$ $x/d>40$
$\frac{f}{f_o} = [1+ 3.5\ \frac{Ra}{Re^{3/2}}]^{.4}$	$300 < Re < 3\times10^4$ $5\times10^3<Ra < 8\times10^6$ $2 < Pr < 6$
$\frac{Nu}{Nu_o} = [1+.031\ \frac{Ra}{Re}]^{1/3}$ $-.15\ \exp[-2(\frac{Ra}{Re}-8)^2]$	$300 < Re < 25000$ $300 < Ra < 8\times10^5$ $2 < Pr < 6$

where:

$$Nu_o = (f_o/8)\,Re\ Pr/k + 12.7\sqrt{f_o/8}\ (Pr^{2/3}-1)$$

$$f_o = (1.82\ \log Re - 1.64)^{-2}$$

$$K = 1 + \frac{900}{Re}$$

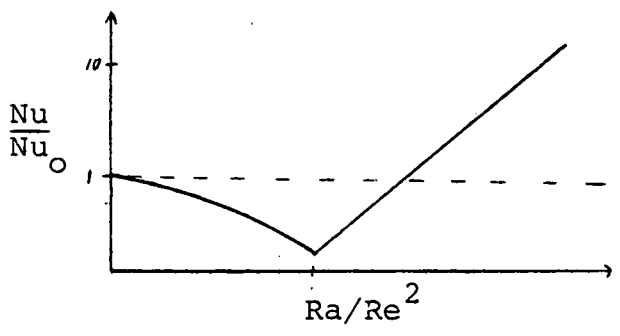

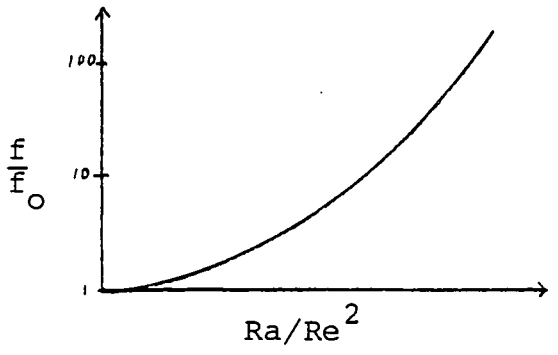

FIGURE 7

Experimental results of Kenning et al (10)

Correlations:

Wall temperature peaking occurs when:

$$Gr_b/Pr_b^{.4}Re_b^{3.4} > 4x10^{-5}$$

Minimum heat transfer coefficient:

$$Nu_f = .75(Gr_f Pr_f)^{.25}$$

Distance for development of wall temperature peak:

$$x/d = .07Re_b^3 Pr_b^{1.2}/Gr_b$$

Data:

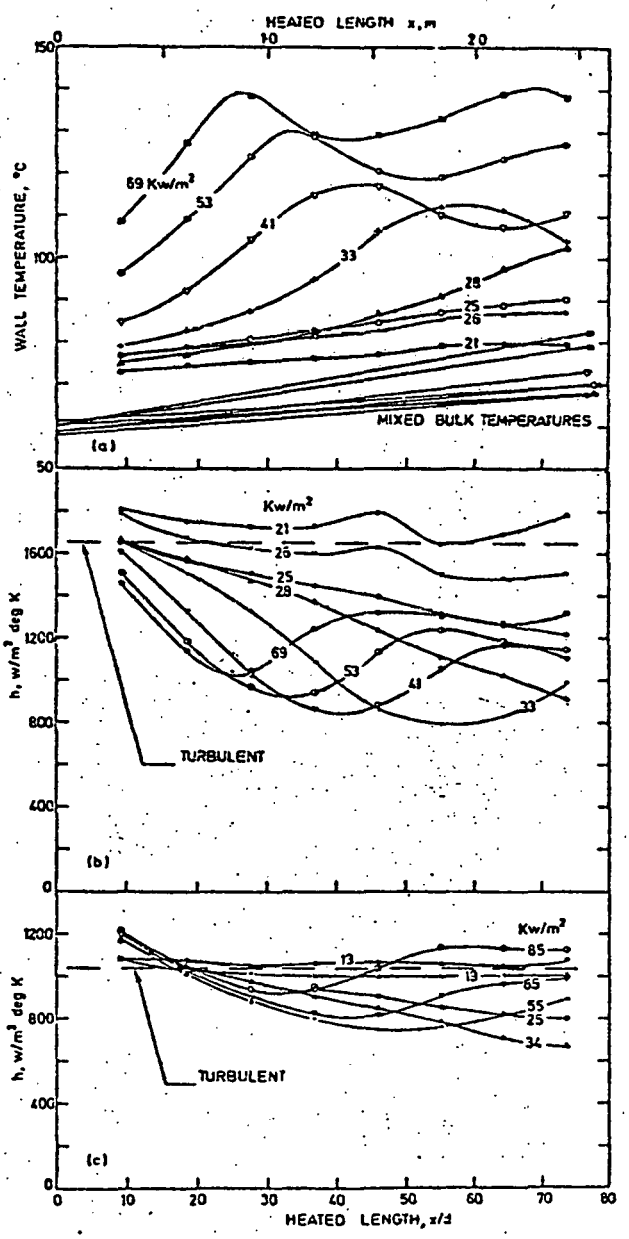

Fig. 1. Axial variations in heat transfer.
a, b 203 kg/m²s, 60°C inlet. $Re_B \approx 16000$, $Pr_B \approx 2.7$.
c 203 kg/m²s, 18°C inlet $Re_B \approx 8300$, $Pr \approx 5.4$.

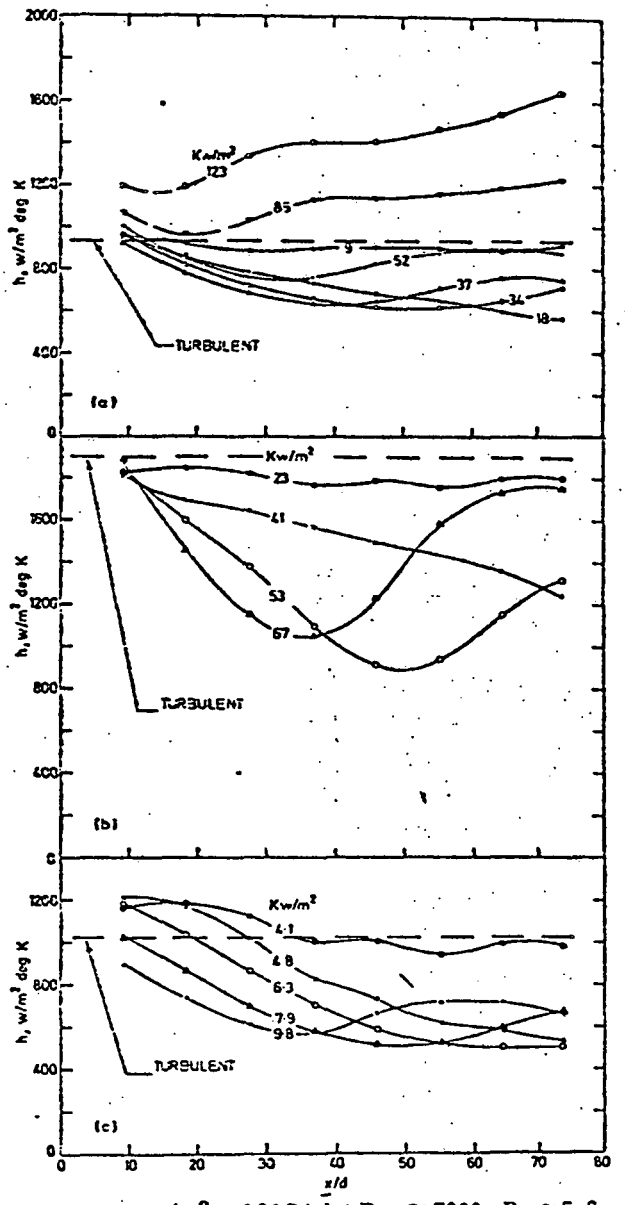

Fig. 2a 180 kg/m²s, 18°C inlet. $Re_B \approx 7000$, $Pr_B \approx 5.8$.
b 255 kg/m²s, 60° C inlet. $Re_B \approx 21000$, $Pr_B \approx 2.6$.
c 122 kg/m²s, 60°C inlet. $Re_B \approx 9100$, $Pr_B \approx 2.8$.

FIGURE 8

Experimental Results of Connor and Carr (14)

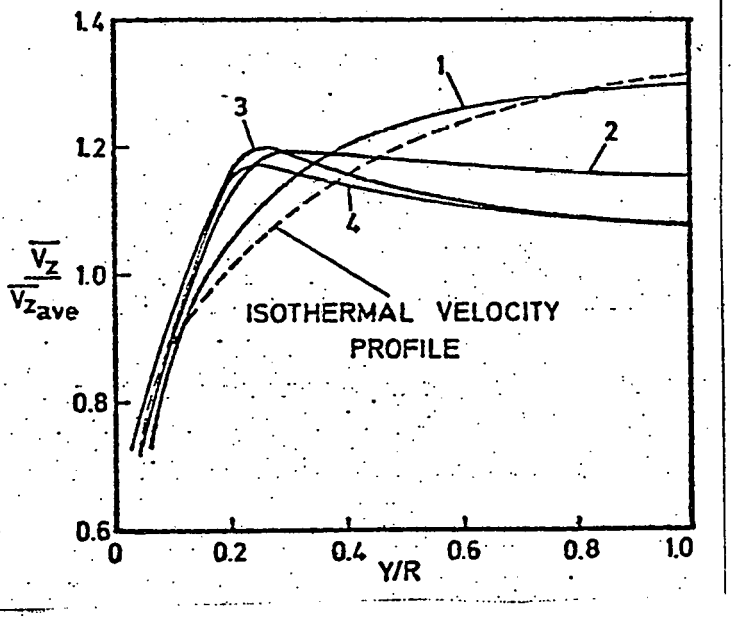

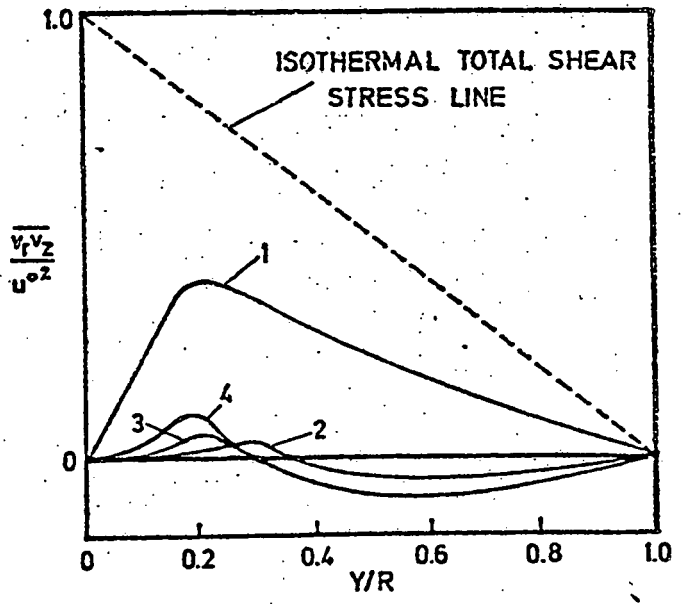

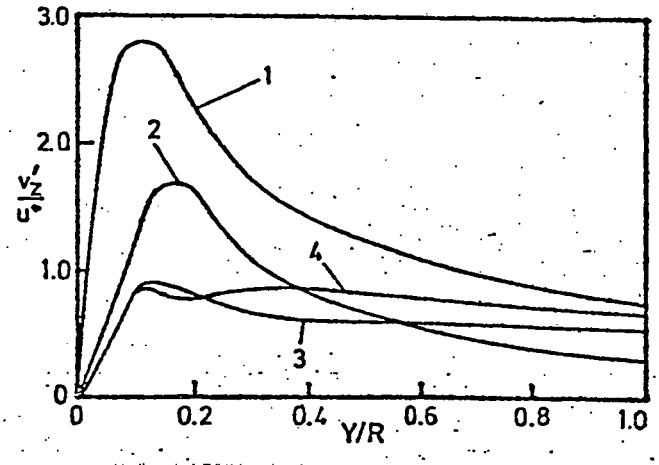

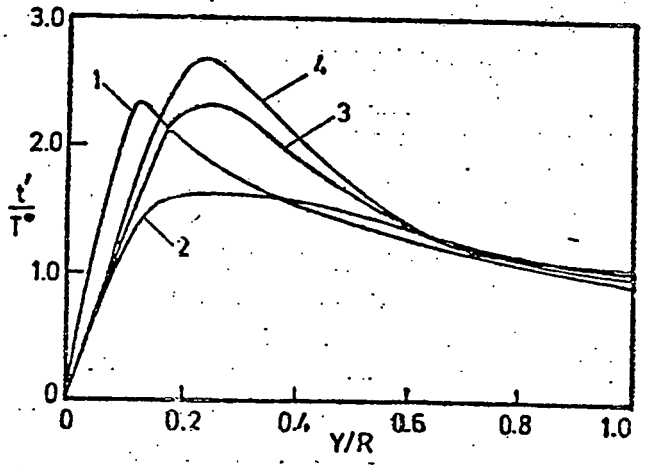

Experimental Results of Byrne and Ejiogu (16)

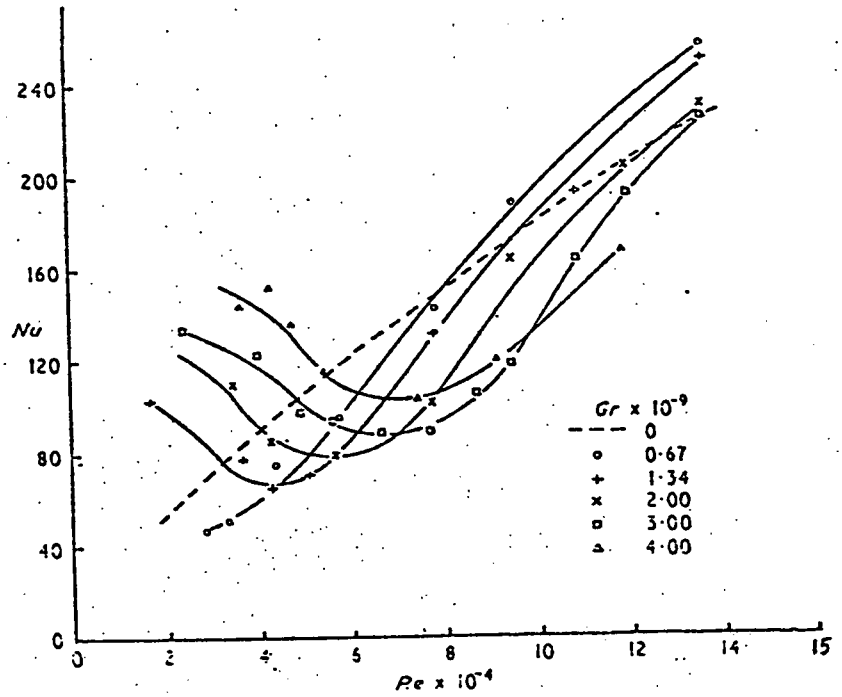

Fig. 118.4. Effect of Grashof number on the heat transfer with forced convection

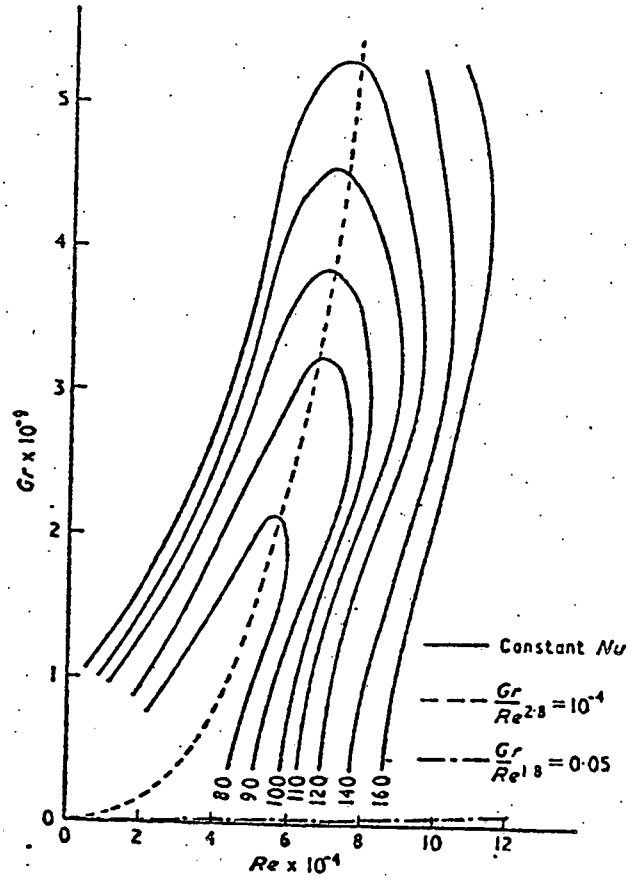

Contours of constant Nusselt number on a grid of Grashof and Reynolds numbers

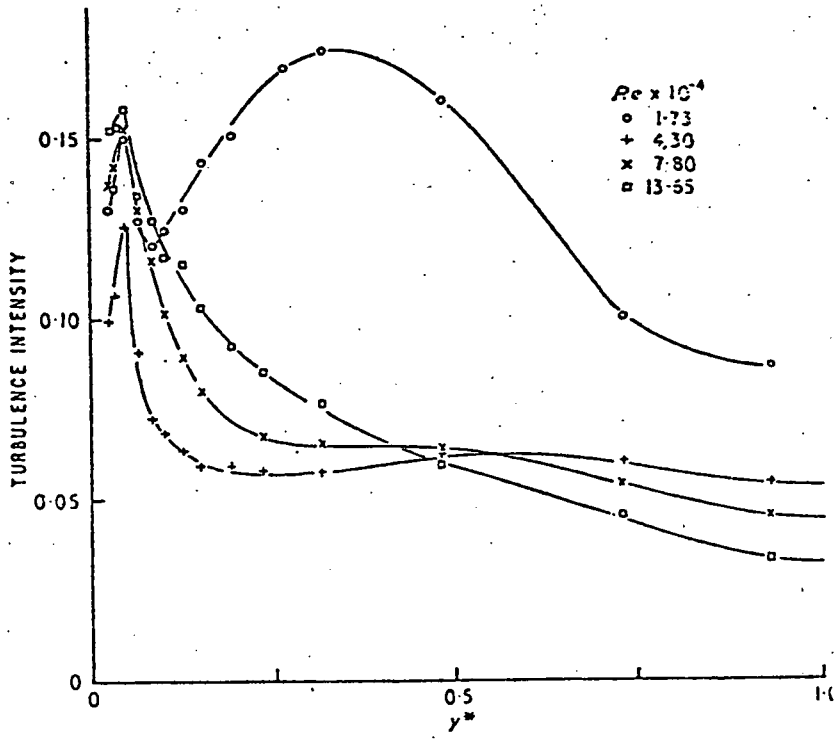

Fig. 118.7. Distribution of turbulence intensity across the pipe at a Grashof number of $1{\cdot}34 \times 10^9$ and various Reynolds numbers

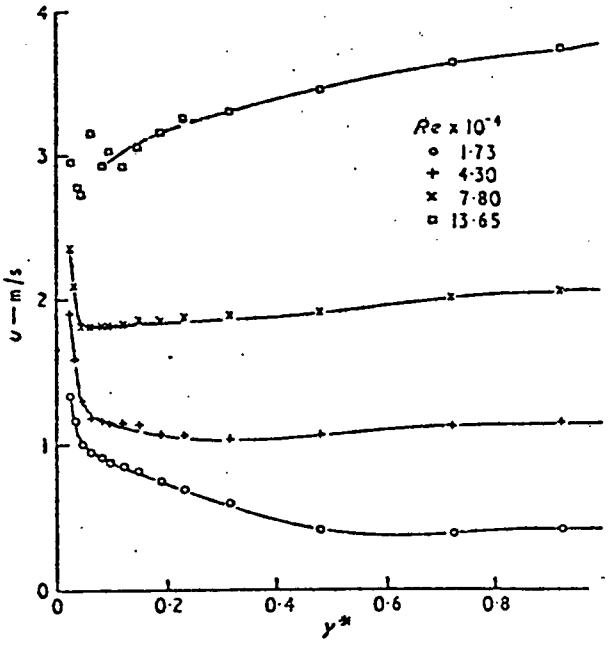

Fig. 118.5. Velocity distribution across the pipe for a Grashof number of $1{\cdot}34 \times 10^9$ at various Reynolds numbers

FIGURE 10

Results of Alferov et al (17)

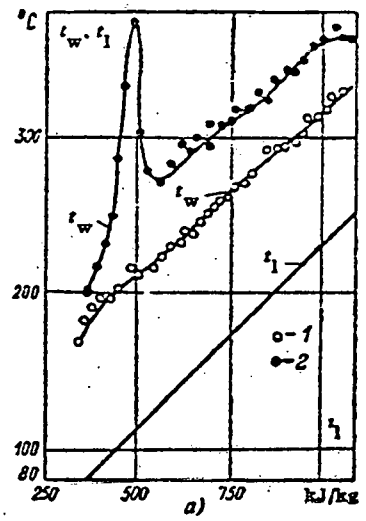

t_w - wall temperature

t_l - bulk temperature

○ - 1 downflow

● - 2 upflow

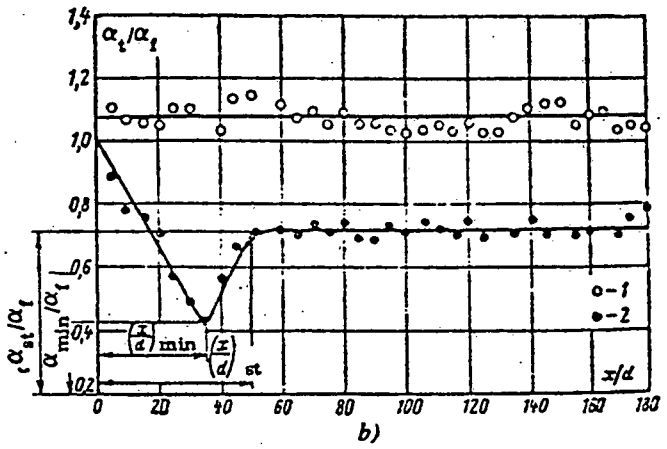

$$(x/d)_{min} = 52(Ra_A/Re)_{in}^{-.5}$$

$$(x/d)_{st} = 1.5(x/d)_{min}$$

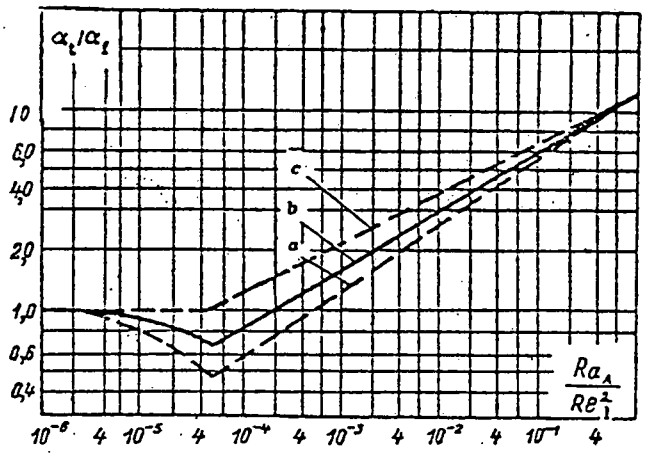

Generalised dependence $\alpha/\alpha_f = f(Ra_A/Re_l^2)$.

curve a - α_{min}/α_f (upflow)

curve b - α_{st}/α_f (upflow)

curve c - downflow

FIGURE 11

Results of Scheele and Hanratty (20)

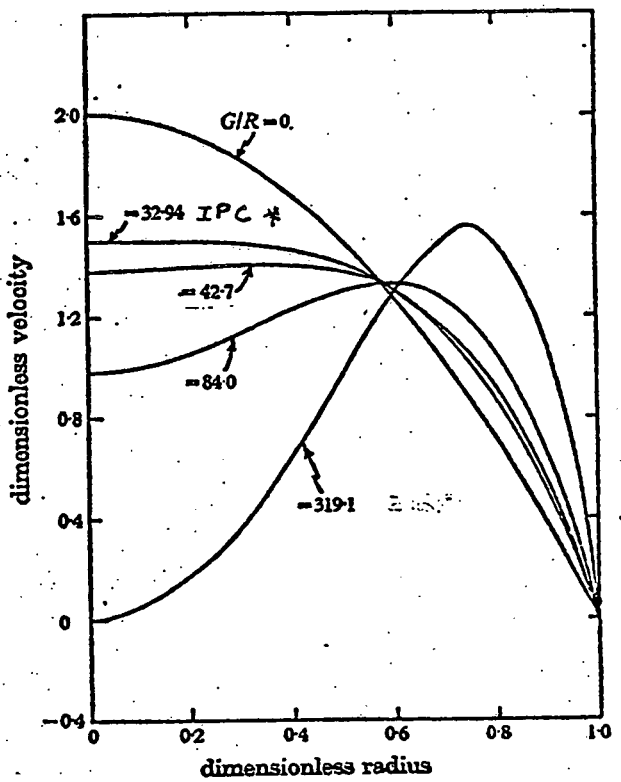

IPC - Inflection Point at the Centerline

IPW - Inflection Point at the Wall

ZGC - Zero Gradient at the Centerline

ZGW - Zero Gradient at the Wall

* - Onset of Instability

Velocity profiles for laminar upflow with constant-flux heating.

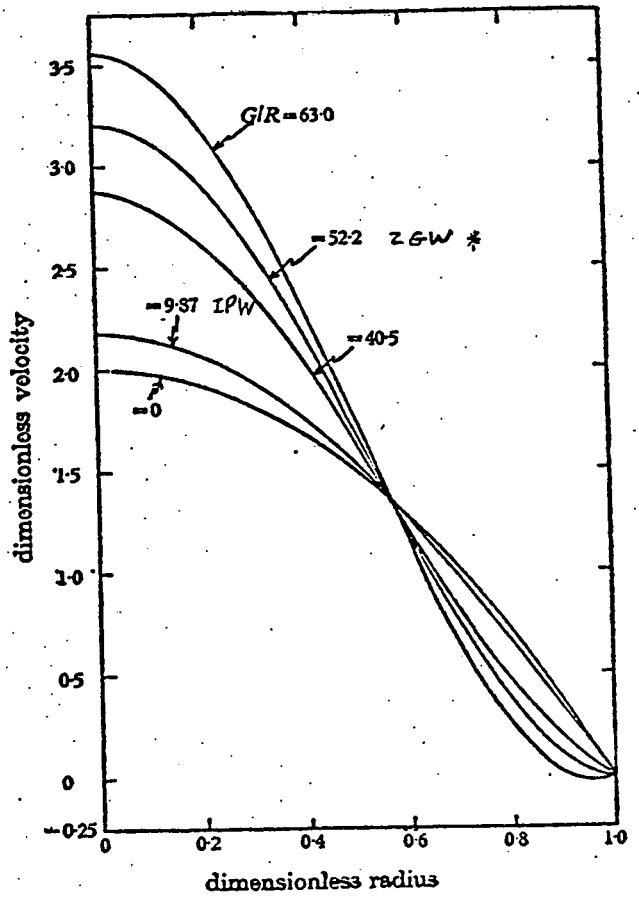

Velocity profiles for laminar downflow with constant-flux heating.

FIGURE 12

Results of Sherwin and Wallis (21)

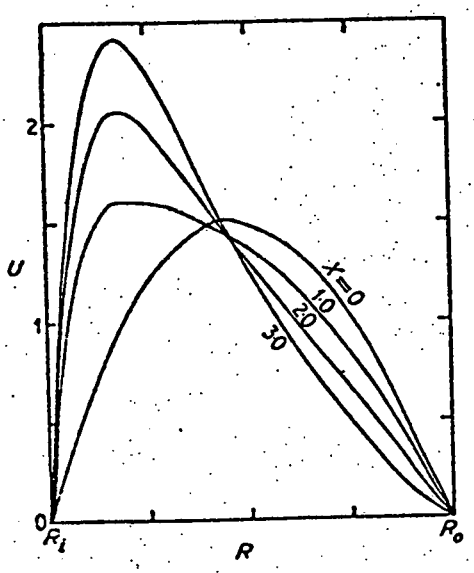

Fig. 12.1. Developing axial velocity profiles—
$Gr_q/Re = 400$

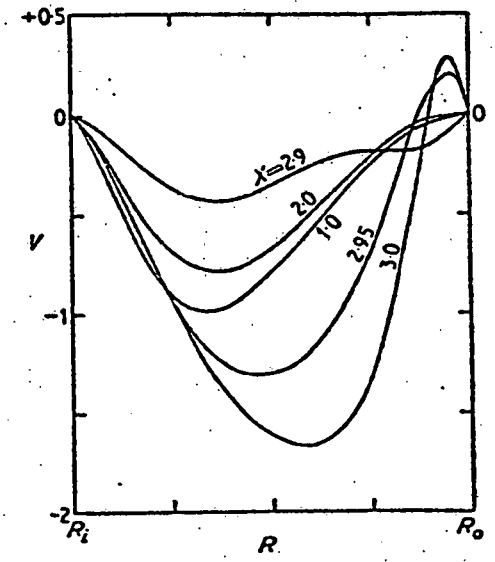

Fig. 12.2. Developing radial velocity profiles—
$Gr_q/Re = 400$

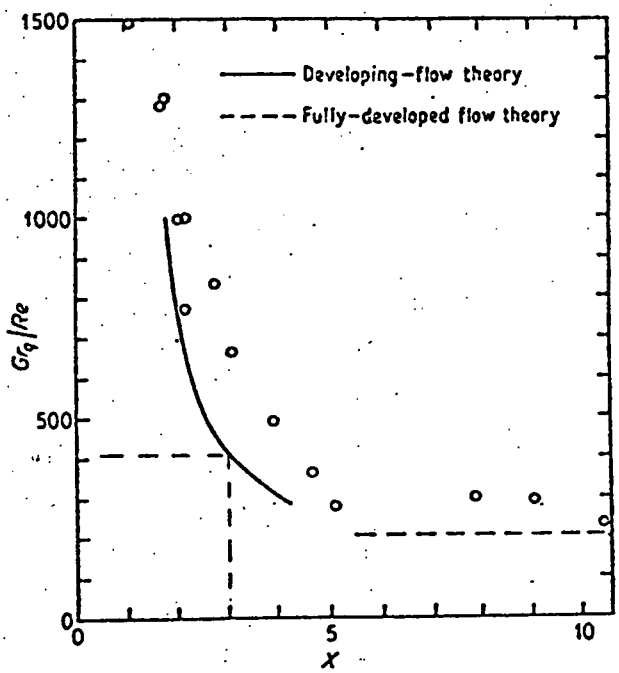

Fig. 12.3. Onset of flow instabilities

$$X = \frac{z/(R_0 - R_i)}{Re}$$

= dimensionless axial distance

FIGURE 13

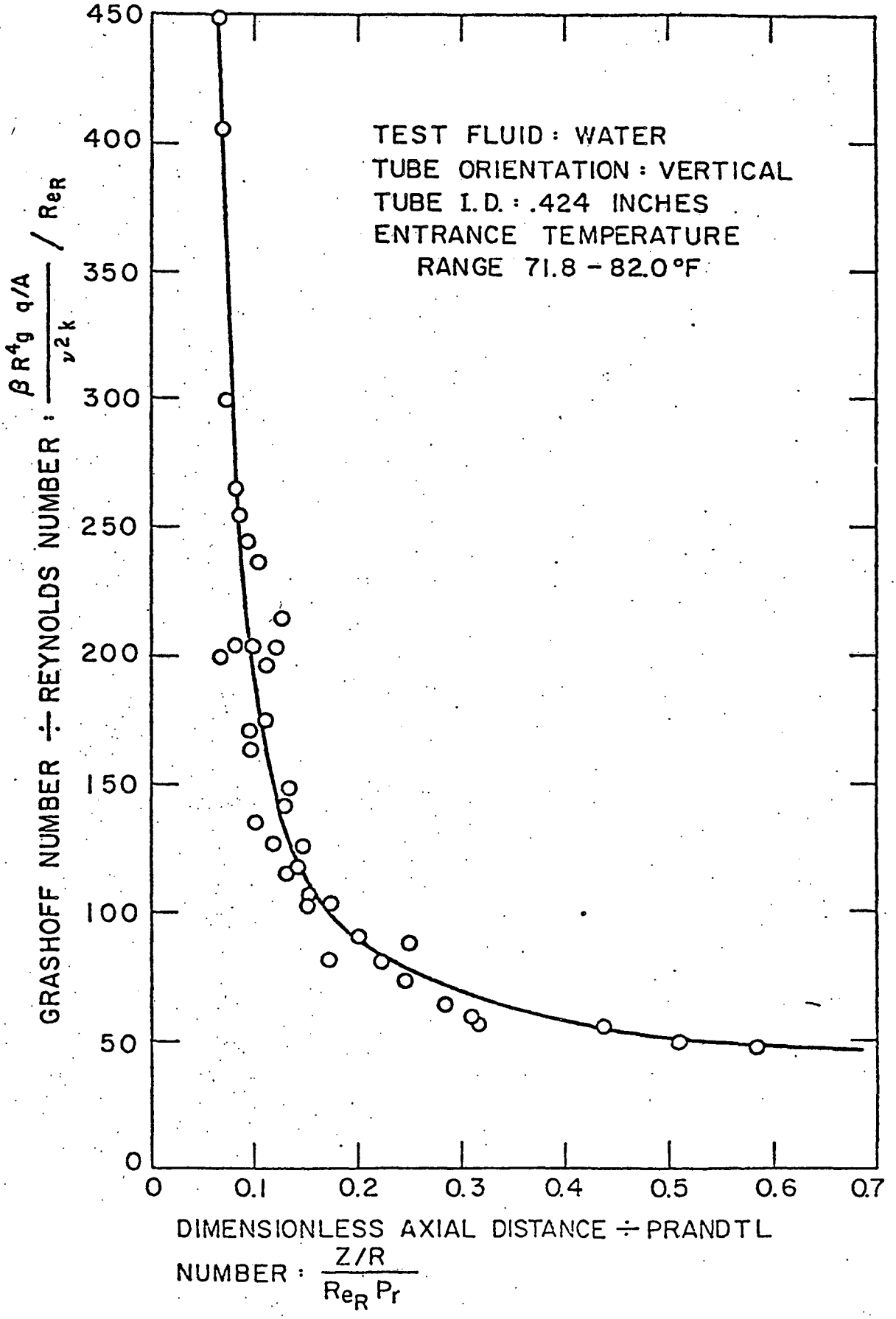

EXPERIMENTAL TRANSITION DATA.

FIGURE 14

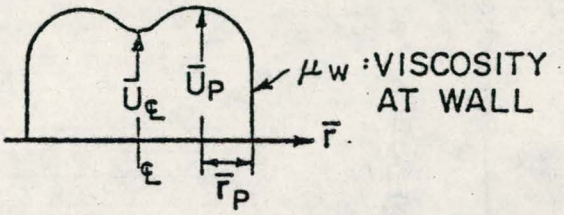

TRANSITION PROFILE NOMENCLATURE
SHOWN ON AXIAL VELOCITY PROFILE

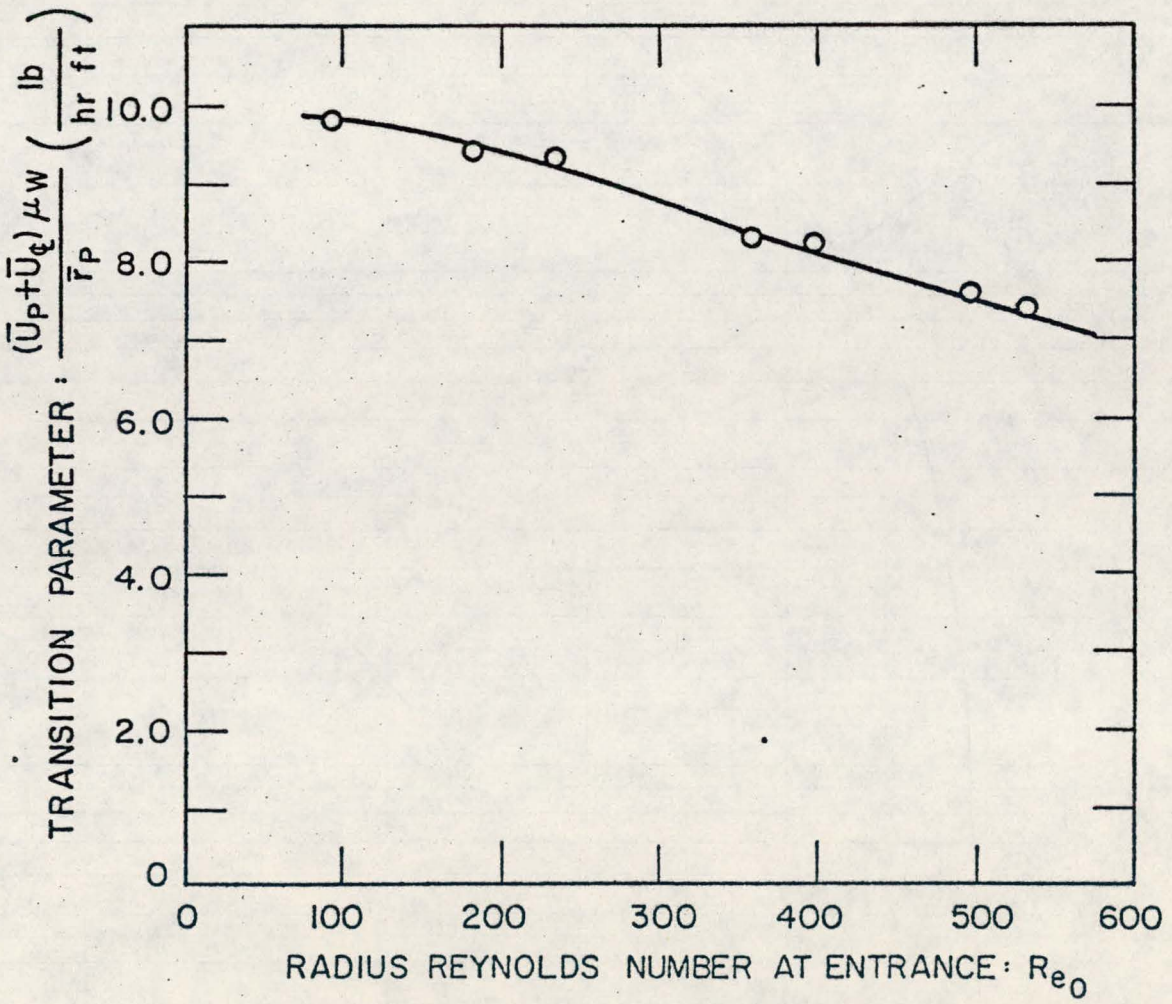

VELOCITY PROFILE SHAPE TRANSITION PARAMETER
AS A FUNCTION OF ENTRANCE REYNOLDS NUMBER.

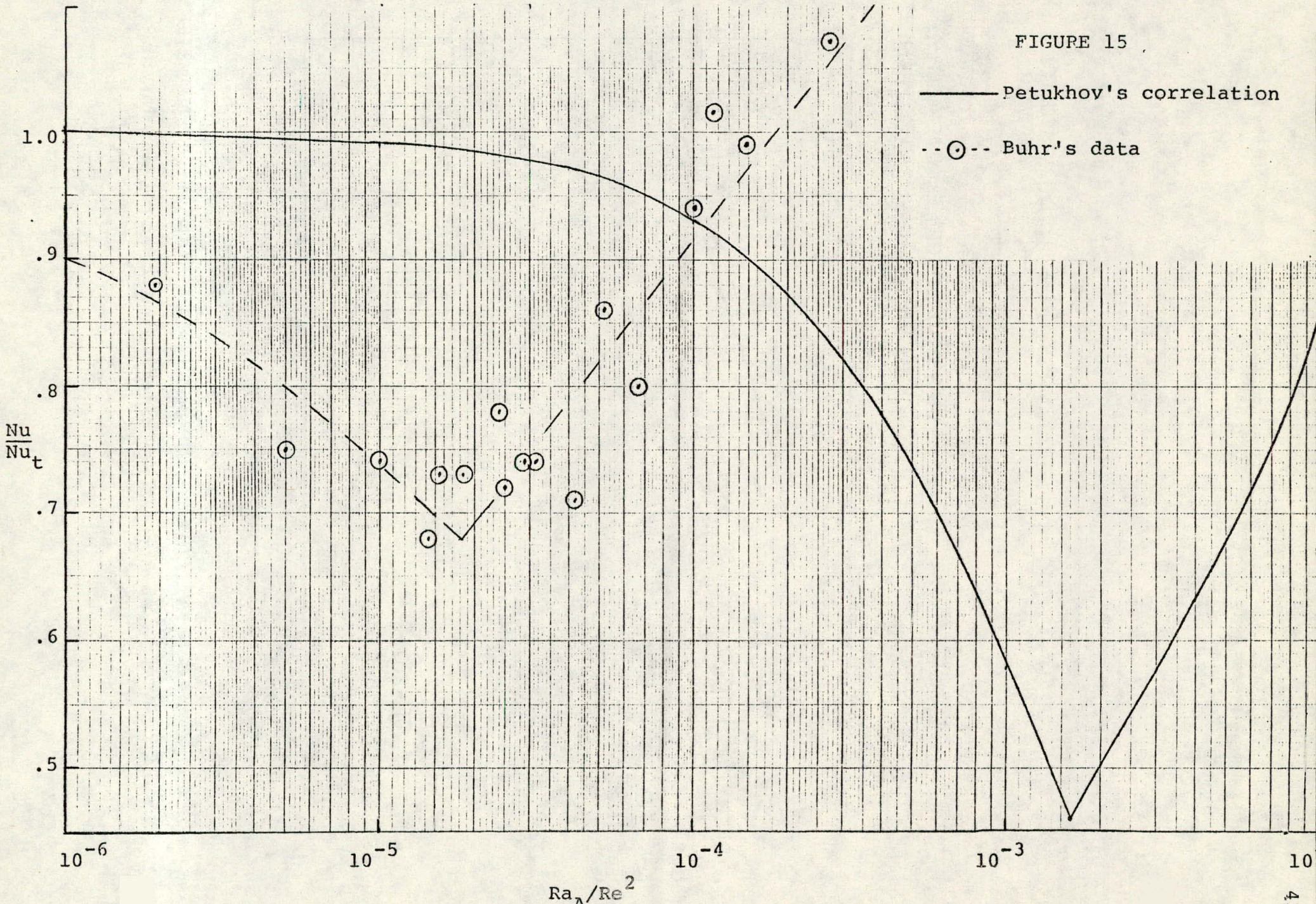
FIGURE 15
Petukhov's correlation
Buhr's data
1.0
.9
.8
.7
.6
.5
Nu/Nu_t
10^-6
10^-5
10^-4
10^-3
10
Ra_A/Re^2

FIGURE 16

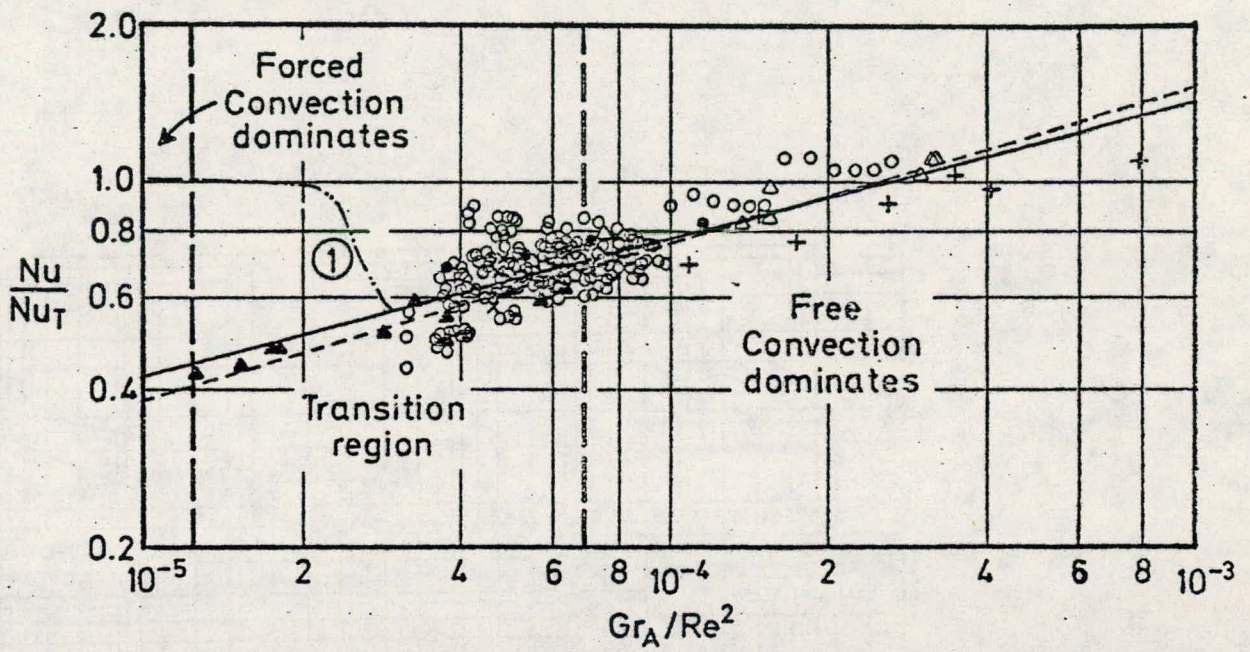

Mixed Convection Nusselt Number Correlation (only Type II flow data are shown)

———— Equation (1) : $Nu/Nu_T = 8.84\ (Gr_A/Re^2)^{0.263}$
– – – – – Estimated line for water data of Petukhov and Strigin
—·—·—·— Curve 1 : Type I flow data from Run 41

Data: Air ▲ Connor
Water O Kenning et al. ; × Alferov et al.
Mercury + Horsten ; Δ Louw ; ● Jacoby

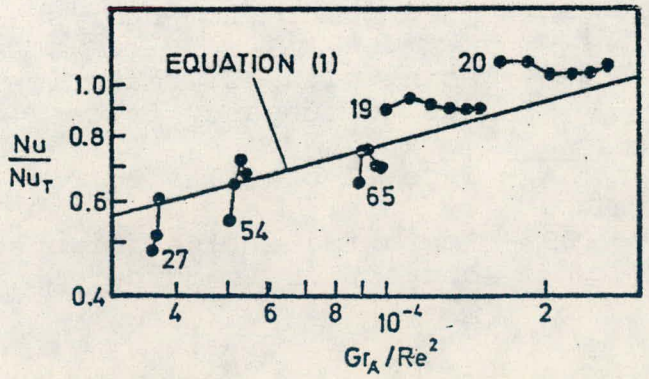

Comparison of Equation (1) with type II flow data from five experimental runs made by Kenning et al. (4). Each chain of points represents a series of measurements along the test section for the run indicated.

FIGURE 17

Flow Regime Map with data points
From Buhr's Murcury test.

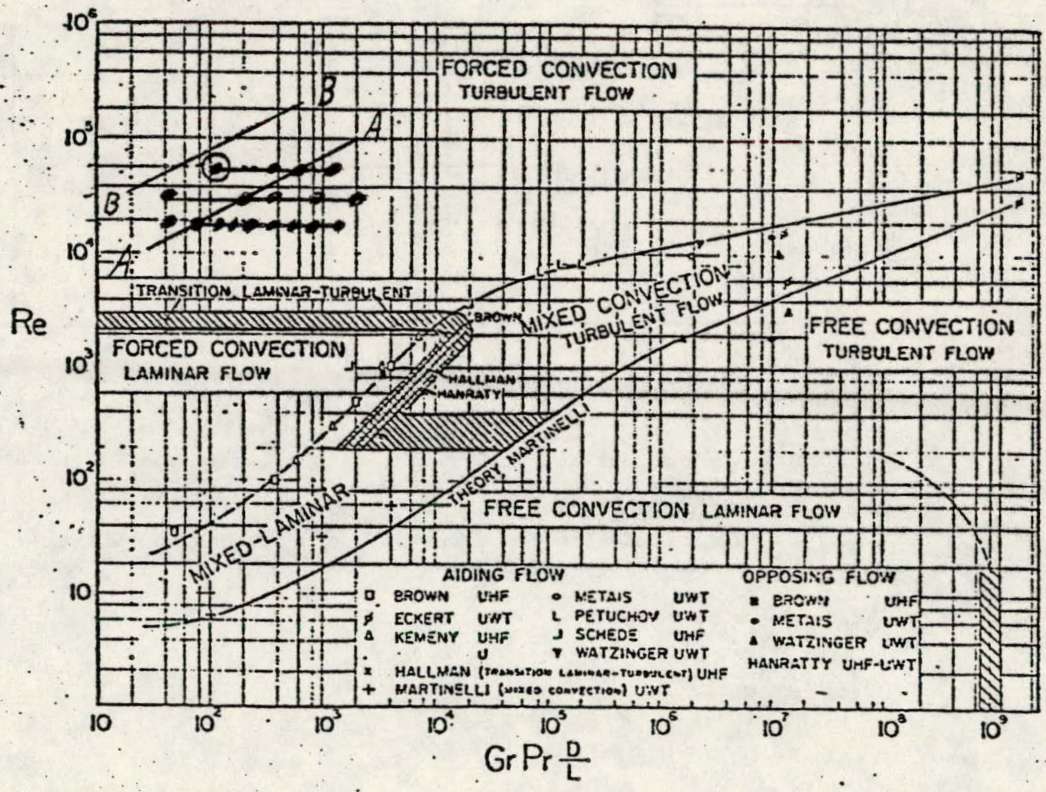

Regimes of free, forced, and mixed convection for flow through vertical tubes

$$\left(10^{-2} < Pr\,\frac{d}{L} < 1\right)$$

—●— - Data point from Buhr's (4) murcury test.

—◉— - Point with 12% reduction in heat transfer due to buoyancy forces.

$\overline{AA}$ - Type II profiles to right of this line.

$\overline{BB}$ - Approximate line for onset of mixed convection in murcury.

FIGURE 18

Kenning's Re=7000 Run

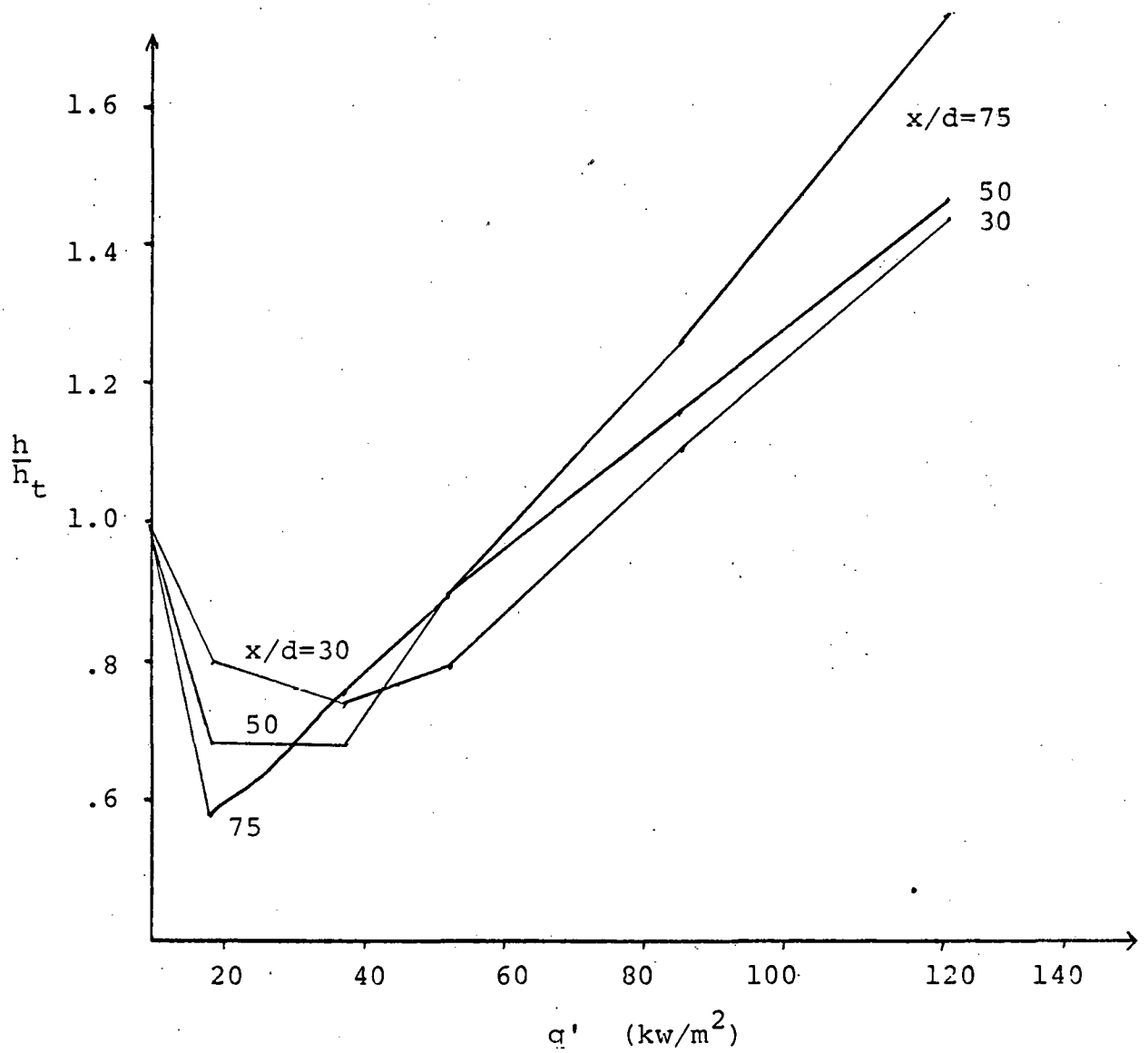

FIGURE 19

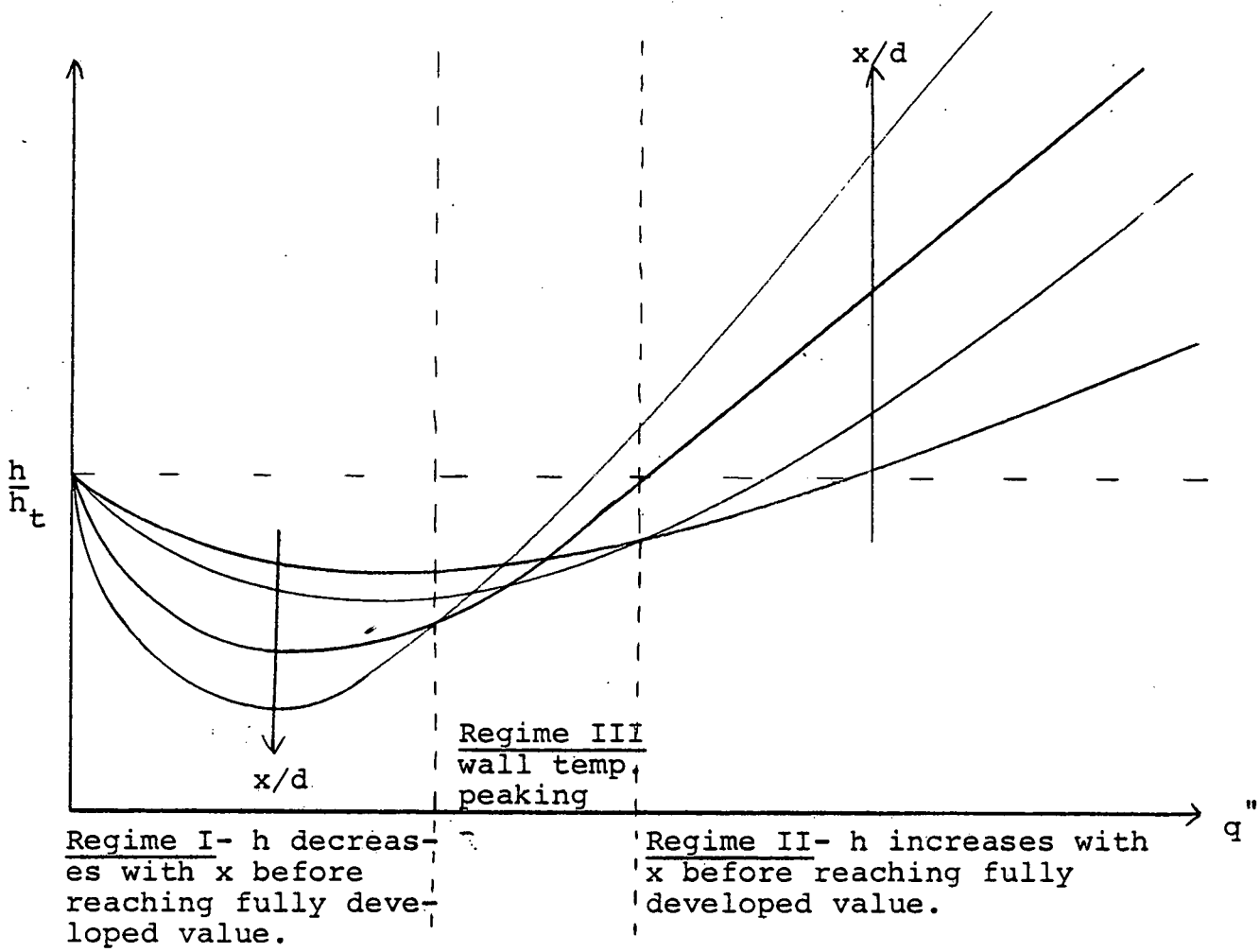
x/d
h/h_t
x/d
Regime III
wall temp
peaking
q"
Regime I- h decreases with x before reaching fully developed value.
Regime II- h increases with x before reaching fully developed value.

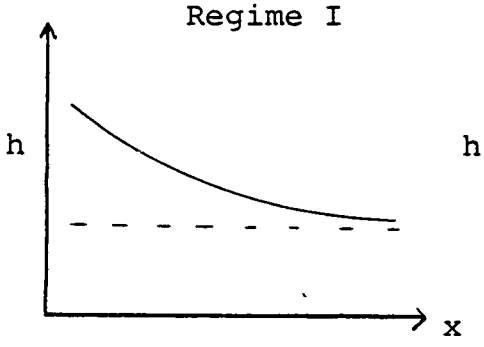
Regime I
h
x

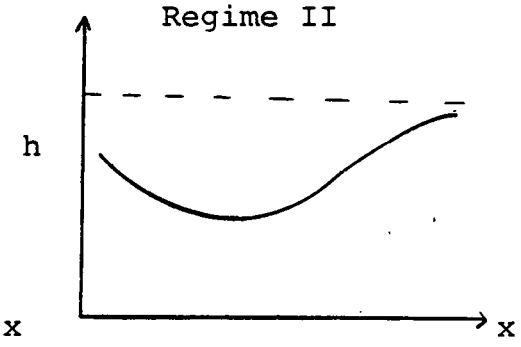
Regime II
h
x

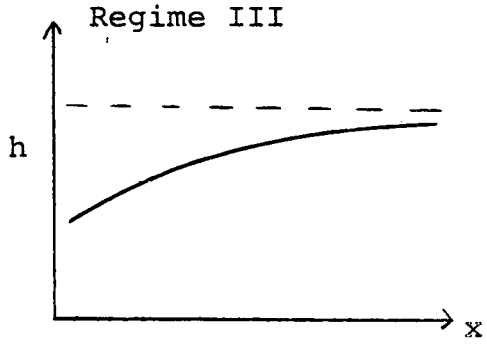
Regime III
h
x

I.D.5 Shape Factors for Transverse Conduction in Rod Bundles

(Sang-Nyung Kim)

During this quarter work has involved setting up the BØDYFIT Computer Code to be used in shape factor calculations. The objective for next quarter is to calculate shape factor from the temperature distribution profile provided by the output of BØDYFIT. This shape factor includes the axial direction variation which represents developing velocity profile effect of entrance. After comparing the outlet temperature distribution between the developing and fully-developed flow, representative values of shape factor will be determined.

TASK II SUBCHANNEL GEOMETRY

This task was completed and last report results appear in Report No. COO-2245-45TR, July 1977 which is listed under B.1 - Original Topical Reports.

TASK III LMFBR OUTLET PLENUM FLOW MIXING

III.A Three-Dimensional Steady Isothermal Flows

(Robert W. Sawdye)

During the period of this progress report the student working in this area was at Battelle Northwest Laboratories working with Dr. D. Trent on TEMPEST development to become more familiar with the code.

III.B Buoyancy Effects and Numerical Treatment of the Convective Equation

(Soon Chang)

The purpose of the work in this effort is to improve the treatment of the advective terms in the fluid flow conservation equations. This effort is motivated by recognition that most of the problems of numerical simulation of fluid flows arise from imperfections in the available treatments.

During this period, the two-step characteristic method has been studied. Basically, there are two different methods of numerical treatment for hyperbolic partial differential equations: the direct finite-difference method, and the method of characteristics. Previous study dealt with donor-cell, interpolated donor cell, central differencing, two-step central differencing and artificial viscosity schemes based on the finite difference method.

Treatment of the convective term in the method of characteristics is dealt with as a method to reduce the effects of truncation errors including numerical diffusion.

Method of Characteristics for the Solution of Turbulent Incompressible Flow in Two Dimension

The method of characteristics generally has been used for the solution of quasi-linear hyperbolic differential equations, governing compressible flow and the flow of small compressibility in one dimension where the sonic characteristic line is considered and diffusion effects are neglected via the Isentropic relation $(\frac{\partial p}{\partial \rho})_s = c^2$, together with the continuity equation, to give the pressure equation. Then the pressure can be calculated along the sonic characteristic line. However, there are several difficulties in the application of the characteristic method to turbulent

incompressible flow in two dimensions which concern this study. First, sonic characteristics can not be used to calculate pressure because the sonic velocity in incompressible flow is infinite. Second, turbulent incompressible flow is subject to turbulent diffusion which can not be dealt with in the classical characteristic method. Third, a difficulty in using the method of characteristics lies in the application to multidimensional cases. In order to overcome the first and second difficulties, a two-step method has been designed. To overcome the third difficulty use of a multidimensional characteristic integral and interpolation scheme is being studied.

The Basis of Characteristic Method

The convection equation in two dimension is as follows:

$$\frac{\partial Q}{\partial t} + u\frac{\partial Q}{\partial x} + v\frac{\partial Q}{\partial y} = 0 \qquad (1)$$

The physical meaning of Eq. (1) is that the transported quantity, Q, remains constant along the characteristic line defined by $\frac{dx}{dt} = u$ and $\frac{dy}{dt} = v$. The method is based upon the determination of these curves, in other words the trace of curve.

Two-Step Characteristic Method

Navier-Stokes equations and continuity equation are as follows:

$$\frac{\vec{u}^{n+1}-\vec{u}^{n}}{\Delta t} + (\vec{u}^{n}\cdot\nabla)\vec{u}^{n} - \nu\vec{\Delta}\vec{u}^{n+1} + \text{grad } p^{n+1} = \vec{f} \qquad (2)$$

and

$$\text{dir } \vec{u}^{n+1} = 0.$$

The above Navier-Stokes equations are separated in the two-step method in the following way.

$$\frac{\tilde{u}-\vec{u}^{n}}{\Delta t} + (\vec{u}^{n}\cdot\nabla)\vec{u}^{n} = 0 \qquad (3a)$$

and

$$\frac{\vec{u}^{n+1}-\tilde{u}}{\Delta t} - \nu\vec{\Delta}\vec{u}^{n+1} + \vec{\text{grad}}\, p^{n+1} = \vec{f}\ , \qquad (3b)$$

subject to

$$\text{div } \vec{u}^{n+1} = 0.$$

Eq. (3a) represents the convection of the momentum and is purely kinematic. Eq. (3b) represents the effect of viscosity or turbulence, pressure and body forces. Eq. (3a) is solved using the characteristic method. Eq. (3b) is solved using finite difference methods. To satisfy the continuity equation, pressure is calculated using MAC method or SMAC method.

Future Work

First, methods to determine the characteristic curve in two dimensions will be studied. This work requires numerical integration and interpolation. Second, the implementation of the two-step characteristic method on the computer code will be done. Third, analytical truncation error analysis of characteristic method will be performed.

References:

J. P. Benque, B. Ibler, A. Kerami, G. Labdie, "A Finite Element Method for Navier-Stokes Equations", Electricite de France.

Y. W. Shin, C. A. Kot, "Two-Dimensional Fluid-Transient Analysis by the Method of Near Characteristics", Journal of Computational Physics, 28, 211-231 (1978).

IV. THEORETICAL DETERMINATION OF LOCAL TEMPERATURE FIELDS IN LMFBR FUEL ROD BUNDLES

Wire-Wrapped Rod Bundle Heat Transfer Analysis

(Chung-Nin Channy Wong)

Introduction

The last progress report (ref. 1) mentioned that a subroutine package which is used to solve the energy equation has been added to the computer code. Results of some calculations have also been discussed. However, this energy-equation-solver utilizes an explicit time differencing scheme for the convection term which has some disadvantages in many cases. An example of this drawback is evident in the analysis of a steady state heat transfer problem without any buoyancy effect. If one excludes the buoyancy effect, one can decouple the momentum-energy equations and solve these two equations separately. Unlike the momentum equation, the energy equation is linear and much easier to solve. So there is no need to treat the convection term explicitly if one is only interested in steady state non-buoyancy effected problems. Therefore, it definitely saves money and time to use a fully implicit energy-equation-solver for some problems.

Fully Implicit Energy-Equation-Solver

The new approach to analyze any heat transfer problem can be found in Figure 1. It is written in a flow-chart form and it illustrates how the present code operates. For those problems without buoyancy effect, a new path has been added. First, the code will check the time control parameter to determine whether this is a steady state or transient problem. If the designated problem is a steady state problem, a fully implicit energy-equation-solver, Subroutine ENERG3, will be used. In ENERG3 both convection and conduction terms will be treated implicitly. The successive over-relaxation (SOR) iterative technique is used to calculate the new temperature. The successive peripheral relaxation (SPOR) iterative technique has been tried but without success. Therefore the SPOR technique has been dropped and the SOR technique adopted.

For the transient problem, there are two choices to be made by the user. If the implicit treatment of the convection term is desired, the code will use the fully implicit energy-equation-solver, ENERG3. However, for the case in which explicit treatment of the convection term is desired, there is another criterion to be determined. It depends upon the Prandtl number. If the Prandtl number

is greater than or equal to one, the heat conduction term can be treated explicitly because the size of the critical time step is still controlled by the explicit treatment of the momentum equation. It is not necessary to use any iteration to update the temperature value. Direct substitution, which is much faster, is good enough. On the other hand, if the Prandtl number is less than one, the conduction term has to be treated implicitly and an iterative method is the technique required to calculate the new temperature.

Result

Two steady state problems have been run and analyzed. The first one is a simple slug flow in a circular duct accounting for the thermal entrance effect. The second one is a hydrodynamically fully developed laminar flow in a circular duct also accounting for the thermal entrance effect. Thus, both problems will have 2D velocity and 3D temperature profiles. To achieve the steady state or equilibrium level, the time is set at a very large value, which is about 100,000 sec.

Figure 2 and Figure 4 present plots of the developing temperature profiles of the slug flow problem and the laminar flow problem respectively. These results

were also used to compare with the fully developed temperature profile obtained from analytical solution. The agreement of these comparisons are satisfactory. Figure 3 and Figure 5 are plots of the Nusselt number vs the axial length. These two graphs (Figure 3 and Figure 5) show that there is a slight difference in the fully developed Nusselt number between the finite difference method and the analytical solution. The difference is about 4.75% for slug flow and 5.5% for laminar flow. This can be explained by two reasons. The first is that a linear extrapolation is used to evaluate the wall temperature. This method will under-predict the value because the curve is parabolic rather than linear near the wall. The second reason is that axial heat conduction is included in the finite difference method whereas analytical technique excludes any axial heat conduction. These two effects will improve the heat transfer and increase the value of the Nusselt number.

Future Work

The development of the computer code Heat Flow 3DT for the bare and wire-wrapped rod bundle geometry will continue. Results and discussions will appear in the next progress report.

References

1. C-N. Wong, "Cooling Mixing in LMFBR Rod Bundles and Outlet Plenum Mixing Transients", Progress Report, June 1980 - August 1980.

2. W. Rohsenow, H. Choi, "HEAT, MASS,AND MOMENTUM TRANSFER", Chapter 7, p 141, pp 163-168, Prentice-Hall, 1961.

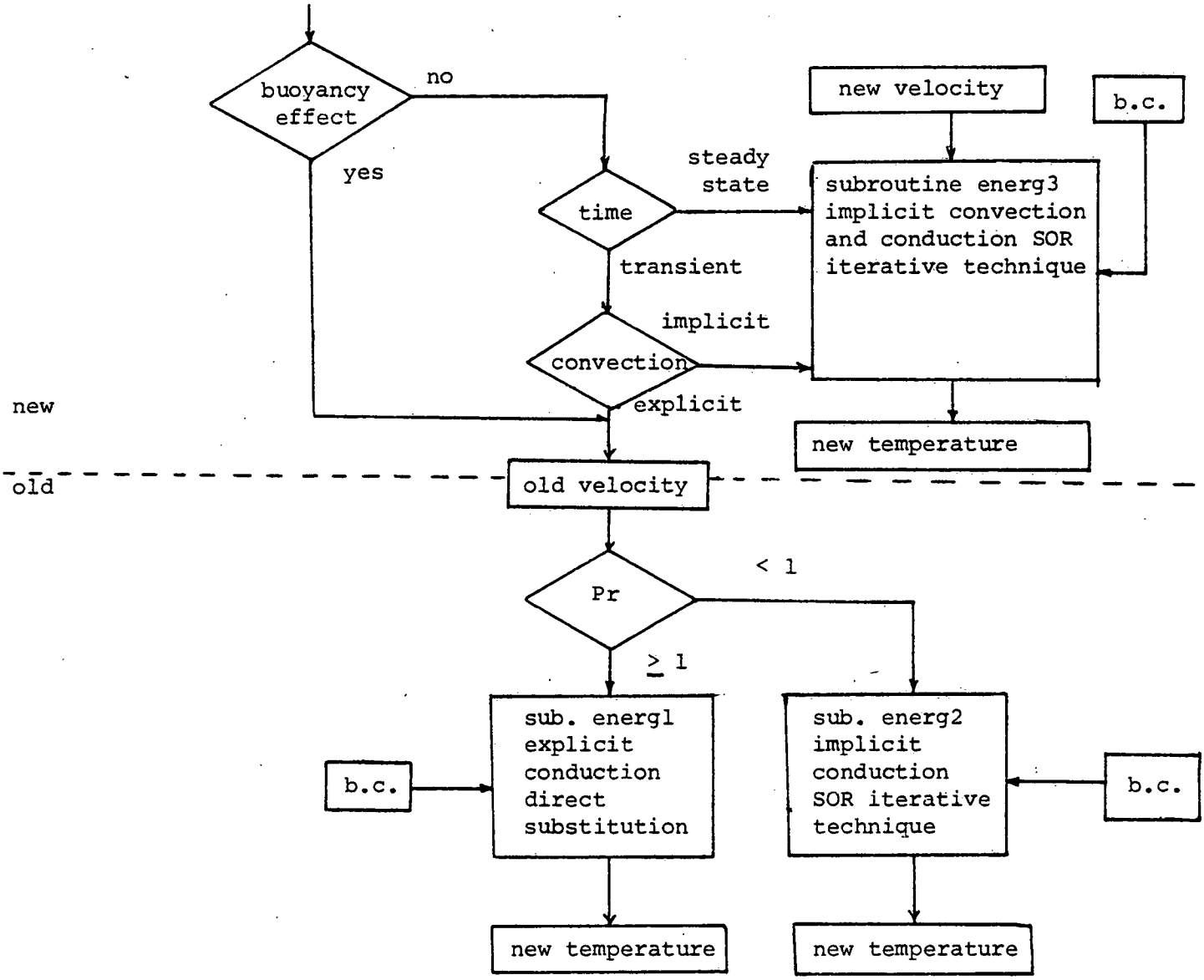

FIGURE 1 Flow Chart of the Energy Solver for any Heat Transfer Problem

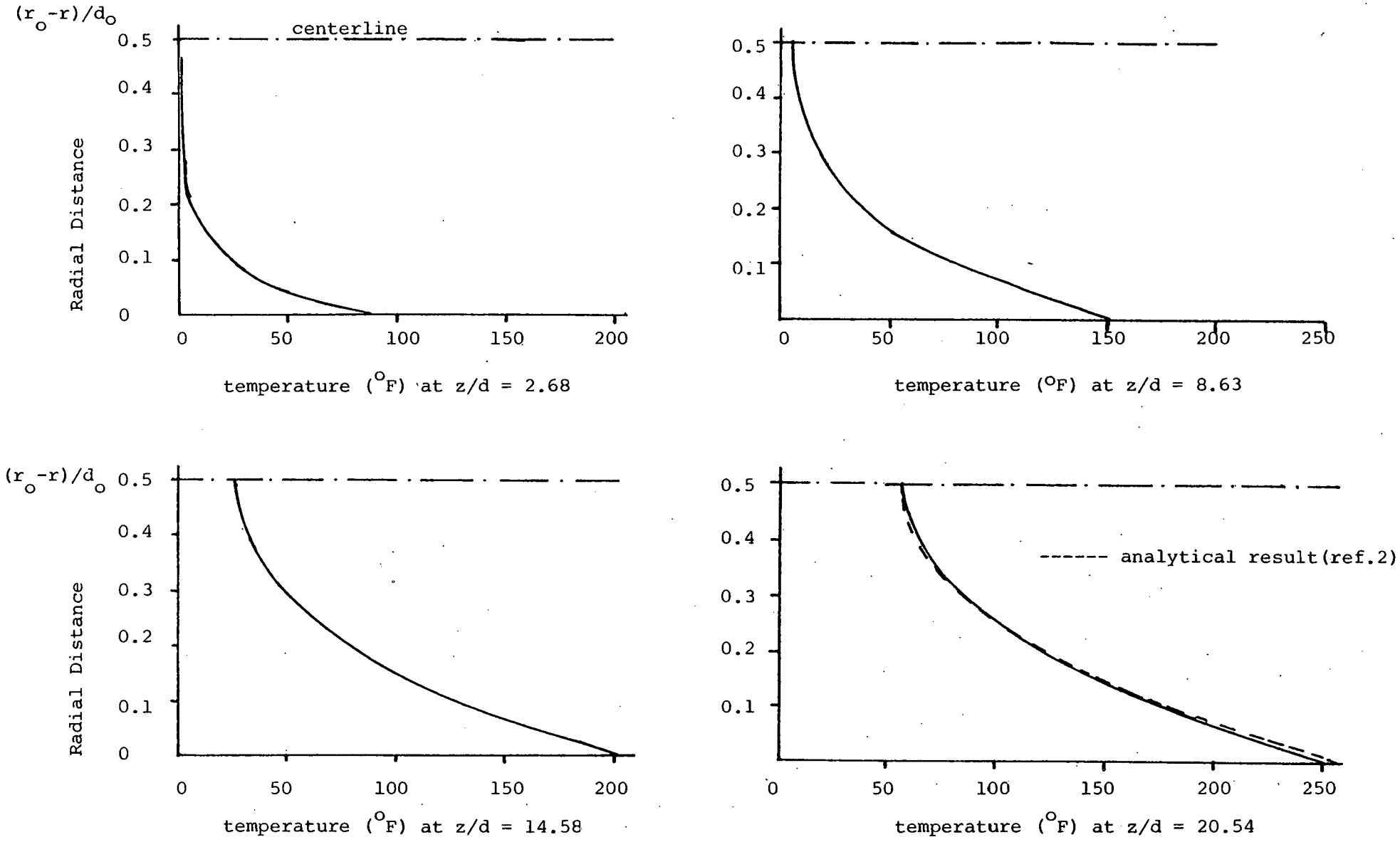

Fig. 2 Temperature Profile of a Heated Pipe at different axial co-ordinates
Slug Flow Dia. = 1" Re = 200 q" = 1 BTU/sec.ft.^{2} water property

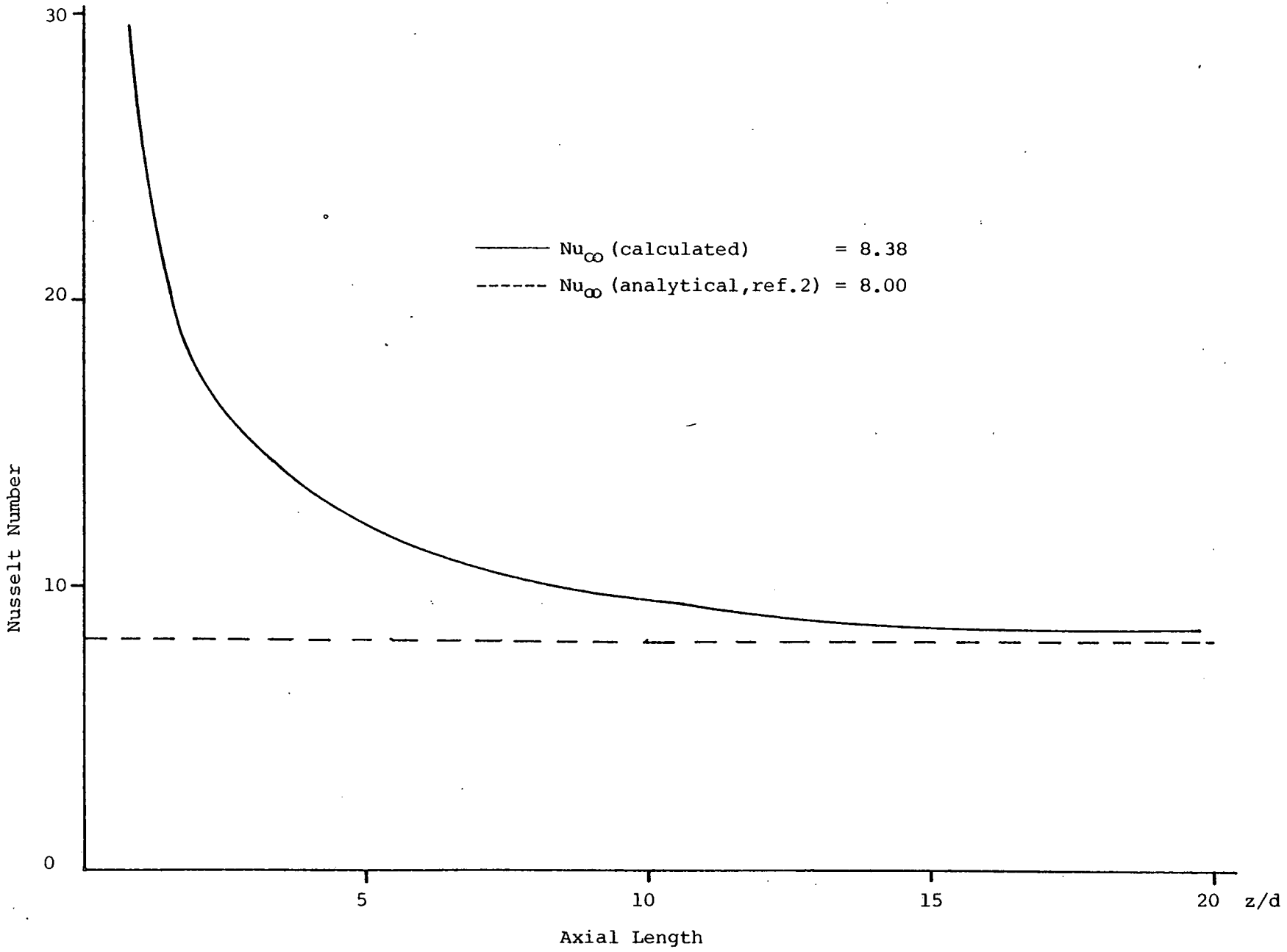

Fig. 3 Nusselt Number vs Axial Length for a Heated Pipe

Slug Dia. = 1" Re=200 q" = 1 BTU/sec.ft.^{2} water property

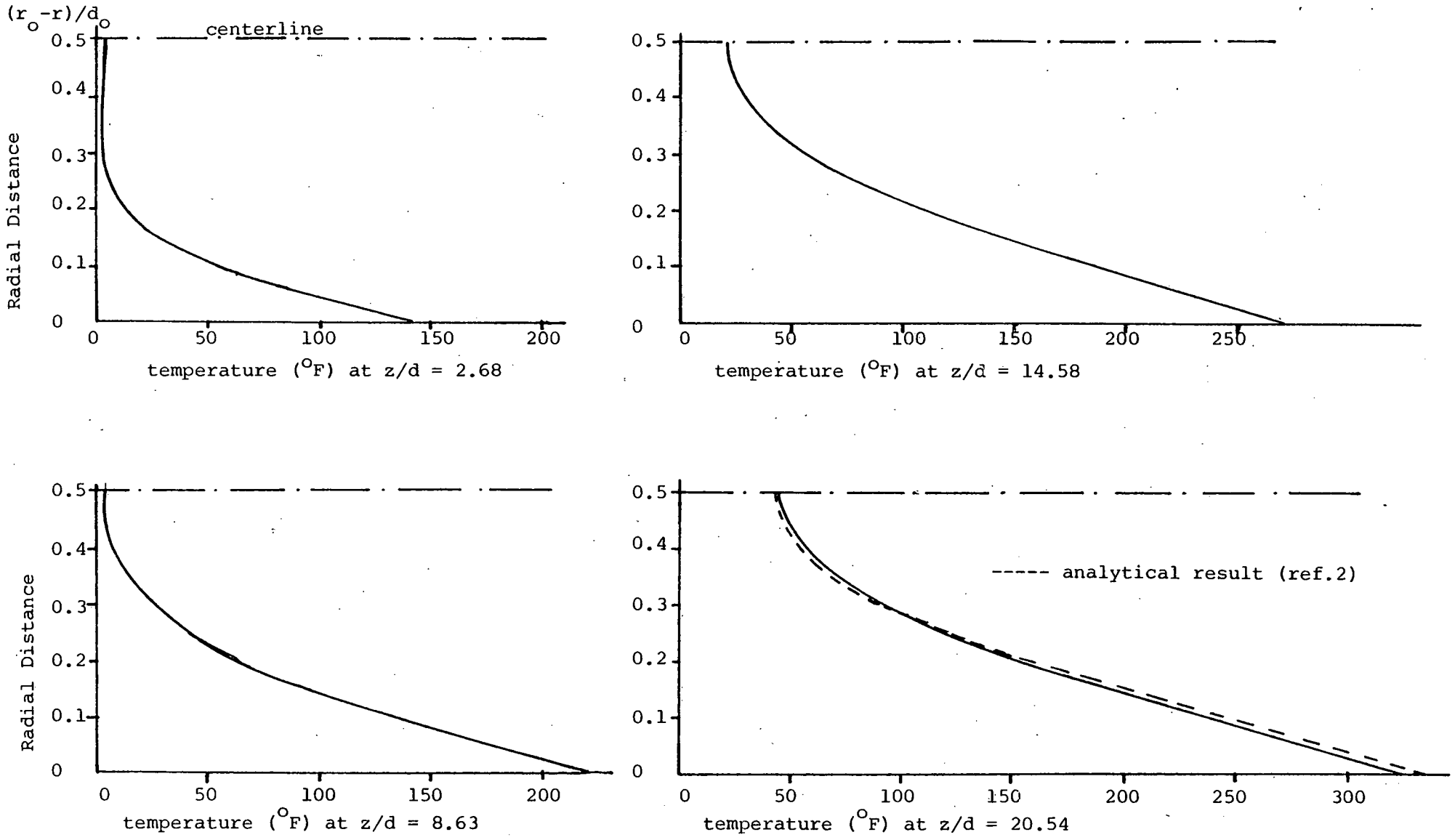

Fig. 4 Temperature Profile of a Heated Pipe at different axial co-ordinates

Laminar Flow Dia. = 1" Re = 200 q" = 1 BTU/sec. ft.^{2} water property

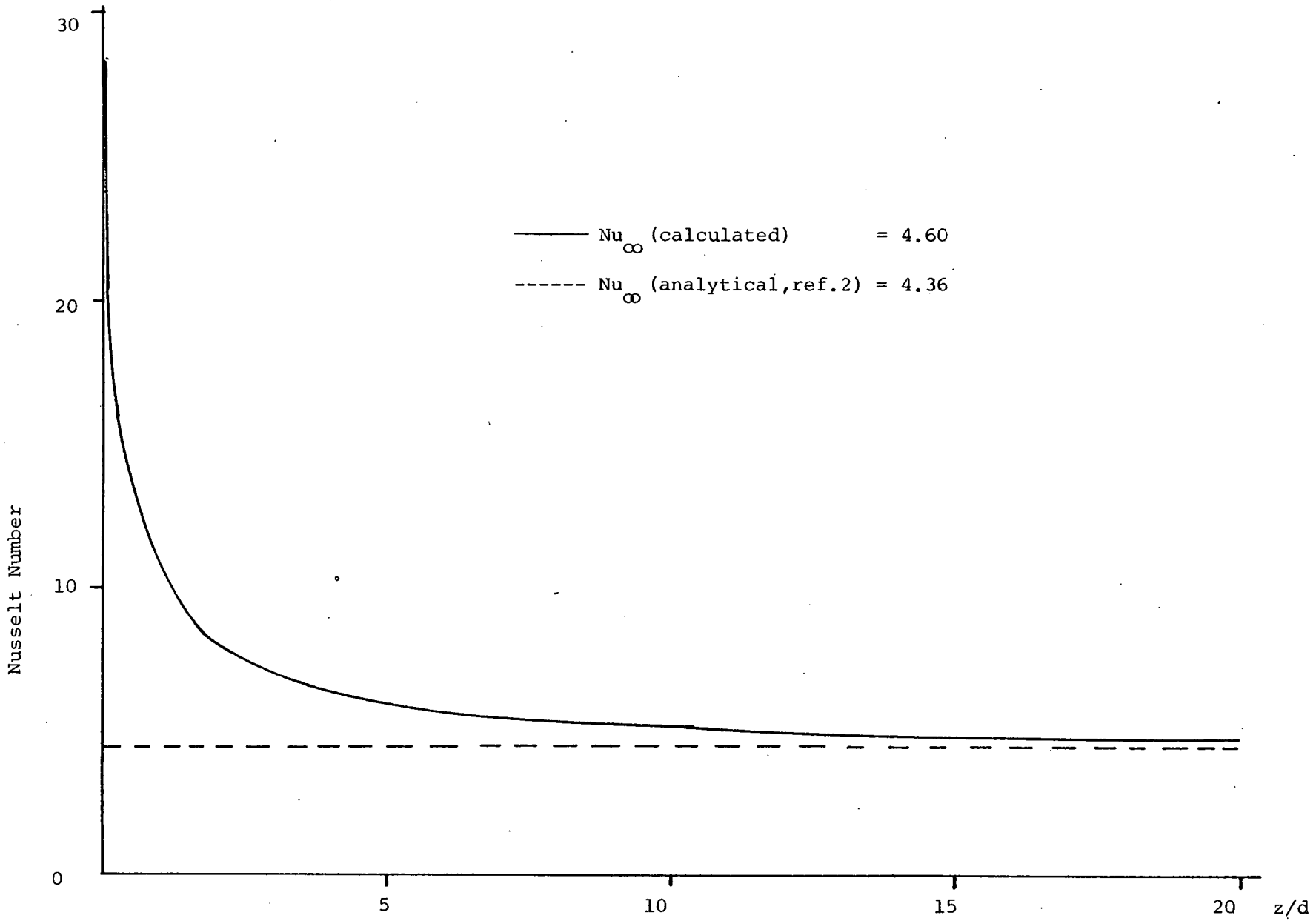

Fig.5 Nusselt Number vs Axial Length for a Heated Pipe

Laminar Flow Dia. = 1" Re = 200 q" = 1 BTU/sec. ft.^{2} water property